International Journal for Parasitology 50 (2020) 873–889

Contents lists available at ScienceDirect

International Journal for Parasitology

journal homepage: www.elsevier.com/locate/ijpara

Identification of critical enzymes in the salmon louse chitin synthesis pathway as revealed by RNA interference-mediated abrogation of infectivity

Laura Braden [a,1,2], Dylan Michaud [a,1], Okechukwu O. Igboeli [a,3], Michael Dondrup [b], Lars Hamre [c], Sussie Dalvin [c,d], Sara L. Purcell [a], Heidi Kongshaug [c], Christiane Eichner [c], Frank Nilsen [c], Mark D. Fast [a,*]

[a] Department of Pathology and Microbiology, Atlantic Veterinary College, University of Prince Edward Island, 550 University Avenue, Charlottetown, PE C1A 4P3, Canada
[b] Sea Lice Research Centre/Department of Informatics, University of Bergen, Thormøhlensgate 55, N-5008 Bergen, Norway
[c] Sea Lice Research Centre/Department of Biological Sciences, University of Bergen, Thormøhlensgate 55, N-5020 Bergen, Norway
[d] Sea Lice Research Centre, Institute of Marine Research, PB 1870 Nordnes, N-5817 Bergen, Norway

ARTICLE INFO

Article history:
Received 26 February 2020
Received in revised form 10 May 2020
Accepted 18 June 2020
Available online 31 July 2020

Keywords:
Salmon lice
RNA interference
Chitin synthesis
Salmon aquaculture
GFAT

ABSTRACT

Treatment of infestation by the ectoparasite *Lepeophtheirus salmonis* relies on a small number of chemotherapeutant treatments that currently meet with limited success. Drugs targeting chitin synthesis have been largely successful against terrestrial parasites where the pathway is well characterised. However, a comparable approach against salmon lice has been, until recently, less successful, likely due to a poor understanding of the chitin synthesis pathway. Post-transcriptional silencing of genes by RNA interference (RNAi) is a powerful method for evaluation of protein function in non-model organisms and has been successfully applied to the salmon louse. In the present study, putative genes coding for enzymes involved in *L. salmonis* chitin synthesis were characterised after knockdown by RNAi. Nauplii I stage *L. salmonis* were exposed to double-stranded (ds) RNA specific for several putative non-redundant points in the pathway: *glutamine: fructose-6-phosphate aminotransferase* (*LsGFAT*), *UDP-N-acetylglucosamine pyrophosphorylase* (*LsUAP*), *N-acetylglucosamine phosphate mutase* (*LsAGM*), *chitin synthase 1* (*LsCHS1*), and *chitin synthase 2* (*LsCHS2*). Additionally, we targeted three putative chitin deacetylases (*LsCDA4557, 5169* and *5956*) by knockdown. Successful knockdown was determined after moulting to the copepodite stage by real-time quantitative PCR (RT-qPCR), while infectivity potential (the number of attached chalimus II compared with the initial number of larvae in the system) was measured after exposure to Atlantic salmon and subsequent development on their host. Compared with controls, infectivity potential was not compromised in dsAGM, dsCHS2, dsCDA4557, or dsCDA5169 groups. In contrast, there was a significant effect in the dsUAP-treated group. However, of most interest was the treatment with dsGFAT, dsCHS1, dsCHS1+2, and dsCDA5956, which resulted in complete abrogation of infectivity, despite apparent compensatory mechanisms in the chitin synthesis pathway as detected by qPCR. There appeared to be a common phenotypic effect in these groups, characterised by significant aberrations in appendage morphology and an inability to swim. Ultrastructurally, dsGFAT showed a significantly distorted procuticle without distinct exo/endocuticle and intermittent electron dense (i.e. chitin) inclusions, and together with dsUAP and dsCHS1, indicated delayed entry to the pre-moult phase.

1. Introduction

Several pathogens compromise the sustainability of global commercial salmon aquaculture, including ectoparasitic copepods (Family: Caligidae). One of the most notorious of these, *Lepeophtheirus salmonis*, is responsible for global economic losses to the industry exceeding USD 1 billion annually (Brooker et al., 2018). The parasite has a direct life cycle that involves eight developmental stages, each separated by a moult (Wootten et al., 1982;

* Corresponding author.
E-mail addresses: lbraden@aquabounty.com (L. Braden), dmichaud@upei.ca (D. Michaud), mfast@upei.ca (M.D. Fast).
[1] First authorship is shared equally.
[2] Current address: AquaBounty Canada, Inc., Canada.
[3] Current address: Department of Biology, Waterloo University, Waterloo, ON N2L 3G1, Canada.

https://doi.org/10.1016/j.ijpara.2020.06.007
0020-7519/

Boxaspen, 2006; Hamre et al., 2013). Pathology associated with infection includes degradation of the epithelia, chronic wounds, osmoregulatory distress, and predisposition to secondary bacterial and viral infections (Wootten et al., 1982; Wagner et al., 2008).

In efforts to control *L. salmonis* infestations, antiparasitic pharmaceutical treatments are often applied with varying success, and with inevitable positive selection pressure on parasite populations to develop resistance (e.g., Carmichael et al. (2013)). Development of resistance is magnified by the scarcity of available drugs licenced for treatment of sea lice, with only five classes currently employed on a commercial scale, and in many countries only 1-3 licenced for use at any given time (reviewed in Aaen et al. (2015)). Furthermore, negative environmental effects of chemical spillover are a legitimate concern for endemic non-target animals such as amphipods and lobsters (reviewed in Urbina et al. (2019)). To circumvent potential non-target animal effects, a new drug, lufenuron (tradename IMVIXA™) has recently been licenced in Chile, which is an in-feed treatment administered to smolts prior to seawater entry. This benzoylphenyl urea (BPU) has been used successfully for the prevention and treatment of terrestrial ectoparasites for over 30 years (reviewed in Merzendorfer (2013)). There are six chemical classes of chitin synthesis inhibitors used for arthropod pest management, with BPUs the most commonly used (Liu et al., 2019). These drugs have been classified as inhibitors of chitin biosynthesis through direct interaction with *chitin synthase 1* (*CHS1*) (Douris et al., 2016), and their success is reflected in the number of different commercialised insecticides that have been applied against many arthropod species (reviewed in Merzendorfer (2013)). Despite their ubiquitous application, the mode of action of BPUs in copepods has not been characterised and appears to differ from that in terrestrial arthropods (Douris et al., 2016; Michaud, D., Poley, J., Koop, B., Mueller, A., Marin, S., Fast, M., 2018. Transcriptomic signatures of post-moult ageing and responses to lufenuron in copepodid sea lice (*Caligus rogercresseyi*), International Sea Lice Conference, 4–8 November, Peurto Varas, Chile; Poley et al., 2018). A recent study demonstrated a measurable effect of lufenuron on the transcriptome of larval *L. salmonis* (Poley et al., 2018), which was associated with abnormal moulting as evidenced by electron microscopy, and eventual death of the animal; however, in this study, transcripts essential in regulation of moulting, including CHS1, were not differentially expressed. More recently, the effects of various BPUs were investigated on larval *L. salmonis* to try and discern the molecular mode of action; however, there was minimal effect on the transcriptome (Harðardóttir et al., 2019a).

The chitin synthesis pathway (CSP) appears to be complete in *L. salmonis*, and recent studies have characterised key enzymes in the pathway such as chitinases (Eichner et al., 2015b), Chitin synthase 1 (CHS1), Chitin synthase 2 (CHS2), UDP-*N*-acetylglucosamine pyrophosphorylase (UAP), *N*-acetylglucosamine phosphate mutase (AGM) and Glutamine: fructose-6-phosphate aminotransferase (GFAT, (Harðardóttir et al., 2019b)). However, the importance of these and other enzymes to overall fitness (and thus infectivity) of *L. salmonis* is not known. Furthermore, as chitin synthesis is a prime target of current and future anti-parasitic drugs, it is necessary to fully characterise this pathway in *L. salmonis*.

GFAT is a rate-limiting cytoplasmic enzyme in the hexosamine pathway, and its activity has been detected in almost every organism and tissue examined (Kato et al., 2002). Recently, a single copy of GFAT from *Lepeophtheirus salmonis salmonis* (*LsGFAT1*) was described which clustered closely with GFAT sequences of crustaceans and insects, forming a sister group to vertebrate GFATs (Harðardóttir et al., 2019b). Expression analysis among developmental stages indicates that expression of *LsGFAT1* is contingent on the instar age, with significant upregulation observed in later stages of the moulting parasite, supporting the conserved function of GFAT as a critical regulator of chitin production.

AGM was first characterised in the mosquito *Anopheles aegypti* and contains three conserved sequence motifs that are conserved from prokaryotes to mammals (Mio et al., 2000). A single copy of AGM was recently characterised in *L. salmonis* with high sequence homology to that of crustaceans and insects (Harðardóttir et al., 2019b), which upon exposure to the BPU lufenuron was upregulated in a dose-dependent manner in *L. salmonis* copepodites (Poley et al., 2018).

UAP is an essential enzyme that catalyses formation of UDP-GlcNAc (Merzendorfer and Zimoch, 2003), and is critical for survival in insects (Arakane et al., 2011). The importance of UAP in chitin synthesis has been demonstrated where in both *Locusta migratoria* and *Bactrocera dorsalis*, knockdown of UAP resulted in reduced levels of chitin (Kato et al., 2006; Arakane et al., 2011; Yang et al., 2015). There is only one UAP in *L. salmonis*, *LsUAP1*, which was found to be maximally expressed towards the end of the instar stage, before a moult (Harðardóttir et al., 2019b), similar to observations in other arthropods (Liu et al., 2013). The functional importance of *LsUAP1* during chitin synthesis is not known.

Chitin synthase is the final enzyme that synthesises chitin from UDP-GlcNAc. Recently, two chitin synthases were described in *L. salmonis* (*LsCHS1, LsCHS2*), with *LsCHS1* expressed in diverse tissues including antenna, intestine and feet in different life stages, while *LsCHS2* is most highly expressed in the intestine of adult lice (Harðardóttir et al., 2019b). Numerous studies have demonstrated the critical function of chitin synthases in insects (Arakane et al., 2004; Lee et al., 2017); however, it is unclear whether the two chitin synthases in *L. salmonis* share functional roles or if they are distinct, similar to insects (Doucet and Retnakaran, 2012). The role of chitin synthases during exposure to CSIs in *L. salmonis* is unclear.

In addition to the production of chitin, arthropod biology is equally dependent on the proper catabolism of chitin during moulting (Doucet and Retnakaran, 2012). The extracellular matrix (ECM) of an insect is heavily modified in various ways to give rise to the desired physical and mechanical properties of the cuticle. This is largely achieved through chitinases and chitin deacetylases (CDAs). The importance of chitinases in *L. salmonis* was investigated recently (Eichner et al., 2015b), with three distinct chitinases (*LsCHI1, LsCHI2* and *LsCHI4*) belonging to the GH18 group of chitinases in the genome of *L. salmonis*. Expression patterns indicated divergent functions during louse development, and knockdown of *LsCHI2* resulted in reduced infection success. CDAs are secreted metalloproteins which have an active role in the management and manipulation of chitin by facilitating the *N*-deacetylation of chitin to form chitosan, a polymer of β-1-4-linked D-glucosamine residues (Cohen, 2010). One major difference between chitin and chitosan involves their differing electrostatic properties which are thought to have major effects on which chitin binding proteins (CBPs) will bind to these polymers. There is little information on CDAs in *L. salmonis*, or the relative importance of the different variants.

Thus, the objectives of this study were to characterise the functional importance of several enzymes that appear to be important in the chitin synthesis pathway of *L. salmonis* by using RNA interference (RNAi) to knock down expression. By probing the chitin synthesis pathway, we show that there are compensatory mechanisms present in the putative CSP of *L. salmonis* that are successful in rescuing the function of chitin synthesis.

2. Materials and methods

This study was completed in two separate experiments at the Sea Lice Research Centre at the University of Bergen, Norway.

The first experiment (Exp. 1) focused on the knockdown of *LsGFAT1*, *LsUAP1*, *LsCHS1*, *LsCHS2* and *LsCHS1+2*. The second experiment (Exp. 2) was conducted to confirm some of the findings of the first, and to expand the focus to include a greater breadth of targets that might impact chitin formation and degradation by knockdown of *LsCHS1*, *LsCHS2*, *LsCHS1+2*, *LsAGM*, *LsCDA4557*, *LsCDA5169*, and *LsCDA5956*.

2.1. Sequence analysis of chitin deacetylases

Established and putative CDA protein sequences for *L. salmonis*, *Drosophila melanogaster*, *Tribolium castaneum*, *Anopheles gambaie*, *Apis mellifera*, *Daphnia pulex*, *Daphnia magna*, *Bombyx mori*, *Eurytemora affinis*, *Tigriopus japonicus* and *Tigriopus californicus* were obtained from BLASTP or tBLASTn versus GenBank (Dixit et al., 2008; Arakane et al., 2009; Muthukrishnan et al., 2012; Supplementary Data S1). Sequences were assigned as putative and utilised if the following criteria was met: E-value $\leq 10^{-50}$ and identity ≥50%. Amino acid sequences were submitted to MEGA X (ver. 10.1.7; Kumar et al. (2018)), aligned using MUSCLE (default parameters; MEGA X) and evolutionary history was inferred using the Maximum Likelihood method and the Jones-Taylor-Thornton matrix-based model (Jones et al., 1992). The bootstrap consensus tree was inferred from 500 replicates (Felsentein, 1985) to represent the evolutionary history. The initial tree was obtained automatically by applying Neighbour topology with superior log likelihood value.

2.2. Culture of L. salmonis

A laboratory strain of *L. salmonis* was maintained on Atlantic salmon (*Salmo salar*) in flow-through 1 × 1 m^3 tanks (34.5 ppt salinity, 10 °C) as previously described (Hamre et al., 2009). Salmon were hand-fed a commercial diet daily (1% biomass). Lice were carefully collected from salmon anaesthetized in methomidate (5 mg/L) and benzocaine (60 g/L). Egg-string pairs were gently collected from gravid female *L. salmonis* and placed into hatching wells. Eggs, nauplii and copepodites were all held in water from the same supply. All experimental procedures were approved by the Animal Ethics Committee, Norwegian Food Safety Authority (approval number 4538) at the University of Bergen.

2.3. Preparation of double-stranded (ds)RNA fragments

Knockdown targets were chosen based on their putative roles in the chitin synthesis pathway (Kyoto Encyclopedia of Genes and Genomes (KEGG): dme00520) and included apparent non-redundant points (*LsCHS1, LsCHS 2, LsGFAT, LsUAP* and *LsAGM*), as well as three putative chitin deacetylases (*LsCDA4557*, *LsCDA5169*, and *LsCDA5956*). Orthologues in *L. salmonis* were identified using sequences obtained from LiceBase (www.licebase.org), and primers were designed using Primer3 (Rozen and Skaletsky, 2000) and included the T7 promoter (TAATACGACTCACTATAGGG; Supplementary Table S1). A negative control with no sequence similarity to *L. salmonis* (CPY185, a cod trypsin gene) was also included. Double stranded (ds)RNA was produced for these genes using a MEGAscript® RNAi Kit (Ambion, USA) following the manufacturer's instructions. Concentrations were measured using a spectrophotometer (Nanodrop ND-1000, Thermo Fisher Scientific, USA) and adjusted to 0.6 μg/μl.

2.4. RNAi

Egg string pairs were collected from gravid female *L. salmonis* and placed in separate wells of a hatching chamber that was bathed in continuous fresh saltwater (7–10 °C). Chambers were inspected twice daily under a dissecting microscope (Olympus SZX12, 0.5x Olympus objective) for evidence of hatching. The moult from nauplii I to nauplii II has been shown to be the most receptive to dsRNA treatment (Eichner et al., 2014). As soon as nauplii I were observed, larvae from all individual wells with nauplii I were pooled and then ca. 20–100 nauplii were gently transferred to microtube lids (Eppendorf) with 150 μl of seawater for dsRNA treatment.

dsRNA fragments (ca. 1.5 μg; *dsCPY, dsGFAT, dsUAP, dsCHS1, dsCHS2, dsCHS1+2, dsAGM, dsCDA4557, dsCDA5169* and *dsCDA5956;* Table 1) were added to each lid (n = 8–10 replicates) of the corresponding treatment group, and incubated at 7–10 °C for 20 h. Larvae were monitored for moulting from nauplii I to nauplii II, evidenced by shedding of exuviae. Once the presence of nauplii II was confirmed, the dsRNA incubation was terminated. The larvae were carefully washed in fresh seawater and transferred back to the hatching wells in pools corresponding to each treatment until moult to copepodites (ca. 4–5 days post-transfer). After moulting to the infective copepodite stage (determined by a change in morphology), lice were either used for an infection trial (three fish per treatment, n = 80–100 larvae on each fish), or transferred to RNA*later* (Ambion, USA) and stored at −20 °C for subsequent validation of knockdown by real-time quantitative PCR (RT-qPCR, n = 2–6 pools per treatment, n = 30–100 larvae in each pool).

2.5. Fish infection

To assess infectivity after knockdown, larvae were collected from each treatment to conduct a challenge experiment. Atlantic salmon (*S. salar*) were held in single aquaria (40 L) with constant flow through (10 °C) such that each fish was completely isolated from others (Hamre and Nilsen, 2011; Eichner et al., 2014, 2015a). For each of the 10 dsRNA fragments, three fish were infected with 80–100 copepodites per fish. Briefly, the water flow

Table 1
Chitin synthesis pathway enzymes in *Lepeophtheirus salmonis* that were targeted by RNA interference, showing the GenBank and Ensembl accession numbers as well as the EC numbers.

Gene	GenBank	Ensembl	EC
Chitin Synthase 1	MH350851.1	EMLSAG00000002853	EC 2.4.1.16
Chitin Synthase 2	MH350852.1	EMLSAG00000007308	EC 2.4.1.16
Glutamine:fructose-6-phosphate aminotransferase	HACA01002388.1	EMLSAG00000000683	EC 2.6.1.16
N-acetylglucosamine phosphate mutase	HACA01026930.1	EMLSAG00000004055	EC 5.4.2.3
UDP-*N*-acetylglucosamine pyrophosphorylase	HACA01023819.1	EMLSAG00000010580	EC 2.7.7.23
Chitinase 1	KM668222.1	EMLSAG00000008812	EC 3.2.1.14
Glucose-6-phosphate isomerase	HACA01017920.1	EMLSAG00000008931	EC 5.3.1.9
Glucosamine-6-phosphate-N-acetyltransferase	HACA01016749.1	EMLSAG00000012864	EC 2.3.1.4
Chitin Deacetylase 2a (CDA4557)	JP311505.1	EMLSAG00000004557	EC 3.5.1.41
Chitin Deacetylase 2b (CDA5169)	JP307148.1	EMLSAG00000005169	EC 3.5.1.41
Chitin Deacetylase 5 (CDA5956)	JP311505.1	EMLSAG00000005956	EC 3.5.1.41

was temporarily reduced to each tank and copepodites were added. For the next 2 h, a 180 μm filter was placed under the outflow of the tank to collect larvae that did not attach.

Development of the infections was followed until chalimus II (13 days p.i. (Exp. 1); and 21 days p.i. (Exp. 2)). Fish were individually euthanized as previously described (Hamre and Nilsen, 2011) and louse numbers were quantified.

2.6. RNA extraction and first strand synthesis

RNA was extracted from copepodites using a modified phenol–chloroform procedure. Briefly, larvae were isolated from RNA*later* with a 100 μm filter. They were transferred to TRIzol® (Thermo Fisher Scientific™, Burlington, Ontario, Canada) reagent and homogenised with 1.4 mm zirconium oxide beads for 30 min at 50 hz (Tissue-lyser, Qiagen). Samples were incubated at 55 °C with 10 μl of proteinase K for 30 min, and then centrifuged for 3 min at 10,000*g*. The supernatant was removed, added to 200 μl of chloroform and incubated at room temperature for 10 min prior to centrifugation at 12,000*g* and 4 °C for 15 min. The aqueous phase was removed and mixed with equal volumes of 70% ethanol prior to being transferred to a RNeasy mini column (Qiagen) for RNA isolation following the manufacturer's instructions and as described previously (Eichner et al., 2014). An optional on-column DNase digestion was included (DNase-free kit, Qiagen). High quality purified total RNA was eluted in 15 μl of ultra-pure water and quantified using a Nanodrop 2000 Spectrophotometer (Thermofisher), and then assessed using Experion™ RNA StdSens Chips (Bio-Rad Laboratories, Hercules, CA, USA) prior to storage at −80 °C until further use. Poor quality RNA samples were excluded from downstream cDNA synthesis (RQI < 7).

cDNA synthesis was completed using a High Affinity cDNA synthesis kit (Exp. 1; Applied Biosystems, Carlsbad, USA), or the Affinity Script cDNA Kit for qPCR (Exp. 2; Agilent Technologies, Texas, USA) with 1 μg of input RNA in 20 μl reactions following the manufacturer's instructions and stored at −20 °C until further use. Potential genomic contamination in samples was excluded by preparing cDNA reactions (pools of 10 samples) without reverse transcriptase (noRT controls).

2.7. RT-qPCR

RT-qPCR was performed to validate knockdown using SsoAdvanced™ SYBR® Green Supermix (Bio-Rad Laboratories Inc, California, USA) according to the manufacturer's instructions in 11 μl reaction volumes. Efficiencies of all primer pairs were determined by performing four-fold eight-point serial dilutions of a cDNA pool created from equal volumes of cDNA from all samples. The specificity of reactions was determined using melting point analysis, with all primer pairs producing a single peak.

Amplification was performed on a CFX Connect Real-Time System (Exp. 1; Bio-Rad Laboratories Inc, California, USA) using the following profile: 95 °C for 30 s, 40 cycles of 95 °C for 5 s, 60 °C for 15 s, and followed by a melt curve of 65–95 °C (in 0.5 °C increments) with a 5 s hold at each increment, or using an Applied Biosystems 7500 Fast Real-Time PCR System (Exp. 2; Applied Biosystems, Carlsbad, USA) with the following thermal regime: 50.0 °C for 2 min, 95.0 °C for 2 min, 95.0 °C of 15 s, 60.0 °C for 1 min for 40 cycles and 95.0 °C for 15 s, followed by a melt curve from 60.0 °C to 95 °C (in 0.15 °C per second increments).

All target genes (Table 2) were normalised to *elongation factor 1α* using the following equations 1–4. Normalised relative quantities (NRQs) were exported to R-Studio (R V3.6.0) for downstream analysis, including correlational analysis, hierarchical clustering and statistical analysis of fold-change differences among groups on a $\log_2$ scale. Statistical differences in expression profiles were determined with a one-way ANOVA followed by a post-hoc Tukey's honest significant difference (HSD) test, with a *P*-value cut-off of <0.05.

RT-qPCR results were analysed with the following equations:

$$Efficiency = 10^{\frac{-1}{Slope\ \ std\ \ curve}} \quad (1)$$

$$\Delta Cq = Cq_{Expermental\ \ gene} - Cq_{Reference\ \ gene} \quad (2)$$

$$Relative\ Quantity = Efficiency^{-\Delta Cq} \quad (3)$$

$$Normalized\ RQ = \frac{RQ_{Experimental}}{Geometric\ mean\ of\ RQ_{Control}} \quad (4)$$

Statistically significant expression differences were detected in GraphPad (V8.2) using a one-way ANOVA followed by a post-hoc Tukey's HSD, with the significance level set at $P < 0.05$ for all comparisons.

2.7.1. Exploratory qPCR

In addition to validating knockdown of the dsRNA targets and genes involved in the CSP, we assessed transcript abundance of enzymes involved in three alternative pathways (*N*-glycosylation, GI anchor biosynthesis, and *O*-GlcNAcylation) to determine the impact of the dsRNA treatments. Transcripts of interest from the three pathways associated with common substrates within the CSP were identified and then curated for the *D. melanogaster* pathway. Full-length coding sequences from *D. melanogaster* were then used in a BLASTn search within the Ensembl metazoa database against *L. salmonis*. Primers were designed for the sequences identified in *L. salmonis* (Table 2) for the GPI biosynthesis pathway: Phosphatidylinositol glycan anchor biosynthesis class A isoform B (*LsPIGA*), Phosphatidylinositol glycan anchor biosynthesis class L isoform C (*LsPIGL*) and Post-GPI attachment to proteins 1 (*LsPGAP1*); *N*-glycosylation pathway: Dolichol-phosphate mannosyltransferase (*LsDPM1*), Mannosyl alpha-1,6-glycoprotein beta-1,2-*N*-acetylglucosaminyltransferase isoform B (*LsMGAT2*), Glucosidase 2 alpha subunit isoform B (*LsGANAB*) and UDP-*N*-acetylglucosaminyltransferase subunit 13 (*Ls*AL*G13*); and the Protein *O*-GlcNAcylation pathway: Glycoprotein-N-acetylgalactosamine 3-beta-galactosyltransferase (*LsC1GALT1*), Polypeptide *N*-acetylgalactosaminyltransferase (*LsGALNT*), Glucosaminyl (*N*-acetyl) transferase 1 (*LsGCNT1*) and Protein O-GlcNAc transferase (*LsOGT*).

2.8. Electron microscopy

Planktonic dsRNA-treated copepodites (dsGFAT, dsCHS1, and dsUAP) and negative controls (dsCPY185) were collected and fixed in Karnovsky's fixative for 48 h at room temperature and then stored at 4 °C until further processing. Samples were removed from Karnovsky's fixative and washed in sodium phosphate buffer (0.2 M; pH 7.2–7.4) twice for 10 min. Lice were then incubated in buffered 1% osmium tetroxide for 1 h at room temperature. After osmification, samples were embedded in low melting point agarose. Following solidification, agar was cut into small cubes. Dehydration in increasing concentrations of ethanol at room temperature progressed from 50% to 100% final ethanol concentration. Each dehydration step lasted 24 h, and each concentration was changed twice. Following dehydration, samples were treated twice with propylene oxide for 1 h at room temperature. Spurr's resin was mixed with propylene oxide in ratio of 1:1 and 1:2. Infiltration took place at room temperature for 24 h for each step. Infiltration with 100% Spurr's resin was carried out under vacuum at room temperature. Finally, samples were embedded in flat bot-

Table 2
Quantitative PCR primers used in this study.

Gene		Sequence (5′-3′)	Efficiency	Product Size (base pairs)	NCBI/Ensembl Accession number	Source
LsEF1α	F	GGTCGACAGACGTACTGGTAAATCC	91.8	229	EF490880.1	Herein
	R	TGCGGCCTTGGTGGTGGTTC				
LsGFAT1	F	AATAGTTGCTGCTCGTCGTG	91.5	210	EMLSAG00000000683	Herein
	R	TCAGAGGCAGAGTCCATTCG				
LsCDA4557	F	GACAGATCGACTTCGGAGCA	98.0	112	EMLSAG00000004457	Herein
	R	TCTGCCGAGAGTCGGAAATAC				
LsCDA5169	F	CTGGTTGCCACATGGTTTCC	93.6	103	EMLSAG00000005169	Herein
	R	GCCCTGTTGGTCTCGAAATG				
LsCDA5956	F	ATCAAGGACATTCGTGGTGGA	94.8	124	EMLSAG00000005956	Herein
	R	GAGCCTTGGATTTGGTGTAGTG				
LsCHS1	F	AGCCTGGACCGTACCTGTAT	95.5	120	EMLSAG00000002853	Herein
	R	TTTAGGCGGTCCTTGATGCG				
LsCHS2	F	GCGTATCTTATGCAGCGGTCT	92.3	91	EMLSAG00000007308	Herein
	R	GAAGGCATCCATCTTCGCCG				
LsAGM	F	ACGATCCTTTGTTCGGCCTTC	92.3	93	EMLSAG00000004055	Herein
	R	TCATACGCCAGTTGATCCGC				
LsCHI1	F	TCCATTCATTTGTACACATGTGGCTTA	102.7	86	EMLSAG00000008812	Sandlund et al., 2016
	R	CATTGTAAGGGTCAAGGAGTCGAAT				
LsUAP1	F	GGAGACACTGTTGGAGCGAT	111.2	228	EMLSAG00000010580	Poley et al., 2018
	R	ATTGGCACCTCTGTCCTTCC				
LsGPI	F	TTGACTCTGCTGGCATTCCT	100.7	194	EMLSAG00000008931	Poley et al., 2018
	R	TCACCAGGGGACTCGTGTAA				
LsAGM	F	TGATGGAGCGAACGGAGTTG	110	101	EMLSAG00000004055	Poley et al., 2018
	R	CCTGGGTTCCGTCGTTGTAA				
LsGNA	F	TTTTGGAAGGTTCCGAGGAG	110.8	166	EMLSAG00000012864	Poley et al., 2018
	R	AAAAAGCCCCGCTCATCATC				
LsPIGA	F	GAGACTCGCCCTTGTCTCTG	96.4	167	EMLSAG00000002370	Herein
	R	CTTTAAGGCGGGGACGAAGT				
LsPIGL	F	CAAATCTCACACGCGACCAC	94.7	196	EMLSAG00000010703	Herein
	R	AGTTCTTCACTCCAACGGGC				
LsPGAP1	F	CCTGGTATATGGGTGTCGGC	99.5	205	EMLSAG00000006071	Herein
	R	AGCGGGTTGTTTGTTCCTCA				
LsDPM1	F	GTGGTCATTATGGACGCGGA	98.9	226	EMLSAG00000006048	Herein
	R	GACGGAAGGAGCCTGTCAAA				
LsMGAT2	F	TCACTGGTGGTGGAAAGCAA	92.6	165	EMLSAG00000010952	Herein
	R	TCACAGTAAGGACACACCCG				
LsGANAB	F	CCTTTGGGGGAAACACGGAC	99.6	220	HACA01027825.1	Herein
	R	ATGAAAGGAACGGCAGCGTAT				
LsALG13	F	ACTCAGTTCGACGCCTTGAT	99.1	196	EMLSAG00000011846	Herein
	R	CTGCCTCTTCAATGTCGGGTA				
LsGCNT1	F	ATGCTCCCTCTAATGTGGGC	97.6	189	EMLSAG00000008816	Herein
	R	TGGGACATTTATCCACGAACC				
LsGALNT	F	ACCCGAAAGAGGGGGTCTTA	93.3	218	EMLSAG00000011685	Herein
	R	GACGACCCTCATCTTGAGCC				
LsC1GALT1	F	TGCCAGCAGTCAAACTCGAT	92.6	118	EMLSAG00000004038	Herein
	R	GCTTTGAGGAACCAATCCGC				
LsOGT	F	TCACGTCAATGCTTCAGATCG	93.0	164	EMLSAG00000004737	Herein
	R	AGCAAACCTTTTTGCCACCAA				

tomed capsules and polymerized overnight in an oven at 60 °C. Cured blocks of samples were cut using an ultramicrotome (Reichert-Jung Ultracut E, Vienna, Austria). Thick sections (500 μm) were stained with 1% toluidine blue solution. Thin sections (80 nm) were stained with uranyl acetate and Sato lead stain. Sections were viewed at 80 kV with an electron microscope (Hitachi TEM 7500, Nissei-Sangyo, Rexdale, Ontario). Images were taken with an AMT HR 40 digital camera (Advanced Microscopy Techniques, Danvers, MA, USA).

2.9. Light microscopy

Prior to being embedded in plastic, samples were fixed in Karnovsky's fixative, and then processed in PBS and a graded ethanol series. The samples were then treated with Technovit/ethanol (50/50) for 4 h (Technovit 7100, Heraeus Kulzer Technique, Germany) followed by overnight treatment with Technovit and hardener. Sections (2 μm) were cut using a Leica RM 2165 microtome, and then stained with toluidine blue (1% in 2% borax) for 1 min and mounted with Mountex (Histolab Products).

3. Results

3.1. Phenotypic aberrations in dsRNA-treated L. salmonis copepodites

After lice had moulted to copepodites and prior to subsequent manipulation, lice in each treatment were observed for irregular behaviour in hatching wells. Lice treated with dsCPY185 (dsCPY; negative control) were evenly distributed throughout the water column and displayed normal phototactic and swimming behaviours, and there was no evidence of irregular morphology compared with untreated controls (Supplementary Movie S1). Similarly, lice treated with dsUAP, dsAGM, and dsCHS2 were observed throughout the water column and maintained positive phototactic behaviour with no irregular phenotypes observed (data not shown).

Lice treated with dsCHS1 were not evenly distributed throughout the water column, with non-motile individuals remaining at the bottom of the hatching wells (Supplementary Movie S2). Upon observation at 4X magnification, the lice appeared unable to maintain proper buoyancy, with their dorsal side flush with the bottom

of the well. Furthermore, dsCHS1-treated lice appeared to be unable to properly fold their swimming legs underneath their posterior segment as seen in the controls (Fig. 1). Their swimming legs were outstretched at an approximate 45° angle. Additionally, in this group, many individuals appeared to have a swollen cephalothorax, although this was not quantified.

Lice treated with the combination of dsCHS1 and dsCHS2 appeared to be unable to maintain buoyancy and were observed lying on the bottoms of the incubation wells with severely compromised swimming ability (Supplementary Movie S3). Similarly, upon 4X magnification, a majority of individuals had dorsal sides flush with the bottom of the well, unfolded swimming legs and swollen cephalothoraxes (Fig. 1).

Lice treated with dsGFAT exhibited a complete inability to swim and were lying on the bottoms of the hatching wells (Supplementary Movie S4). At 4X magnification we observed significant phenotypic irregularities in these animals, including irregularly shaped secondary antennae and a shortened, bloated cephalothorax (Fig. 1).

Lice treated with dsCDA4557 and dsCDA5169 did not differ from controls in their swimming patterns or morphologies (data not shown). In contrast, the dsCDA5956-treated group appeared to have the most prominent phenotype. This phenotype closely resembled that of dsCHS1, where swimming legs were outstretched and mobility was non-existent, and any movements were limited to a 'twitch-like' behaviour that did not produce directional movement in the water (Supplementary Movie S5, Fig. 1).

3.2. Infectivity potential of dsRNA-treated L. salmonis copepodites

To determine the effect of RNAi treatment on infectivity of *L. salmonis* larvae, Atlantic salmon were exposed to dsRNA-treated copepodites (ca. 80–100 per fish). During the exposure protocol, the outflow for each tank was diverted through a 180 μm mesh filter to collect unattached larvae. We then calculated the number of lice still remaining in the system for each treatment which was used to determine infection success (N_{inf}) using the formula:

$$N_{inf} = \left[\frac{a\theta}{b\theta - c\theta}\right] * 100\% \quad (5)$$

where,

$a\theta$ = number of chalimus II

$b\theta$ = number of copepodites used for challenge

$c\theta$ = number of copepodites collected after 2 h

We observed a substantial loss of larvae from tanks (i.e., larvae were flushed from the tank or were unable to attach to the fish), irrespective of the treatment. However, compared with the dsCPY control (28.0 ± 13.4), there were significantly more lice lost in the dsCHS1 (67.0 ± 22.5), dsCHS1 + 2 (56.7 ± 29.0), dsGFAT (95.3 ± 8.1), and dsCDA5956 (68.0 ± 22.1) treatments (Fig. 2). The infectivity potential was calculated as the proportion of chalimus II found attached to fish that remained in the system during the infection challenge (i.e., that were not flushed from the system within 2 h). The negative control group (dsCPY) had an infectivity potential of 29.7 ± 7.3%. Comparatively, dsUAP-, dsAGM-, dsCHS2-, dsCDA4557- and dsCDA5169-treated lice were not significantly different with 26.1 ± 8.7%, 26.0 ± 9.8%, 22.0 ± 1.7%, and 26.0 ± 1.7%, respectively (Fig. 2). In contrast, dsUAP-, dsCHS1-, dsCHS1+2-, dsGFAT-, and dsCDA5956-treated lice had significantly compromised infectivity potential with 12.7 ± 3.1%, 0%, 0.17 ± 0.4 1%, 0%, and 0%, respectively (Fig. 2).

3.3. Microscopy of dsRNA-treated L. salmonis

Scanning electron microscopy was performed on a subset of planktonic copepodites from Exp. 1, dsGFAT, dsCHS1, dsUAP and dsCPY, to examine knockdown impacts on ultrastructure of integument and underlying epithelium. Control (dsCPY) copepodids exhibited an electron dense epicuticle and a procuticle with clear demarcation of the more external exocuticle from the more internal endocuticle (Fig. 3A). The exocuticle/endocuticle, as described previously (Bron et al., 2000a,b; Poley et al., 2018), form overlying lamina of electron dense chitin microfibrils. Control copepodites also showed the presence of an ecdysial membrane and early signs of exuvial cleft formation, suggesting they had entered the early stages of proecdysis or pre-moult (i.e. D_0-D_1). Mitochondria, endoplasmic reticulum (ER) and other organelles were observed directly below the epithelial border with the extracellular matrix (EM), also suggestive of maintained cuticulogenesis.

Similar to dsCPY, organised overlying laminar chitin within the procuticle was evident in both dsUAP (Fig. 3B) and dsCHS1 (Fig. 3C). However, in dsGFAT (Fig. 3D) the procuticle was distorted and the exo- and endocuticle were difficult to distinguish, with disorganised inclusion of electron dense, likely chitinous, material. The dsCHS1- and dsGFAT-treated animals did not exhibit a clear ecdysial membrane or early formation of the exuvial cleft as in dsCPY, but appeared more similar in nature compared with the dsUAP, which showed an electron dense apical membrane with the presence of ecdysial droplets and formation of electron dense vesicles, which in some cases appeared to fuse with the apical membrane (Zhao et al., 2019).

Light microscopy revealed structural differences among the different treatment groups compared with controls (Fig. 4). The dsCPY controls were characterised by intense staining and internal structures including bands of striated muscle. dsGFAT-treated lice appeared to have less chitin in their exoskeleton compared with dsCPY or dsCHS1, as indicated by very light toluidine blue staining, with the interior of the louse also staining very lightly with pockets of empty space. Furthermore, there was evidence of old cuticle without the new cuticle present in the dsGFAT group and their new cuticle was much less pronounced than that of dsCPY controls or dsCHS1-treated lice. The cuticle of thickened malformed appendages observed macroscopically in dsCHS1 and dsGFAT (Fig. 1) were characterised by foci of light blue staining (Fig. 4B, C).

3.4. Sequence analysis of CDAs

Maximum likelihood analysis was completed for various arthropod and copepod putative CDAs using MEGA X with 500 bootstrap replicates. *LsCDA4557* contains three conserved domains; a chitin-binding perithrophin-A domain (CBD), a low-density lipoprotein receptor class A domain (LDLa) and a CDA catalytic domain, which are characteristic of group I CDAs (CDA1s and CDA2s; Fig. 5A). After phylogenetic reconstruction *LsCDA4557* clustered closest to other copepod sequences (*TjCDA2, TcalCDA2, EaCDA2* and *LsCDA5169*) and together formed a sister clade to CDA2s identified in arthropods (Fig. 5A). Sequence analysis revealed that *LsCDA5169* contains only LDLa and CDA domains and is missing a CBD characteristic of group I CDAs. However, the current sequence available for putative *LsCDA5169* (JP307148.1) from the Transcriptome Shotgun Assembly (TSA) database of NCBI appears to be a partial sequence and thus may be the reason for the absence of a CBD. *LsCDA5956* clustered strongly with copepod CDA5s, *TjCDA5* and putative *TcalCDA5* (group 4; Fig. 5), which together formed a sister group to other CDA5s from Insecta and Branchiopoda. Similar to *LsCDA5169*, *LsCDA5956* (JP311505.1) is also a partial sequence and is missing a CBD and linker region characteristic of CDA5s. Thus,

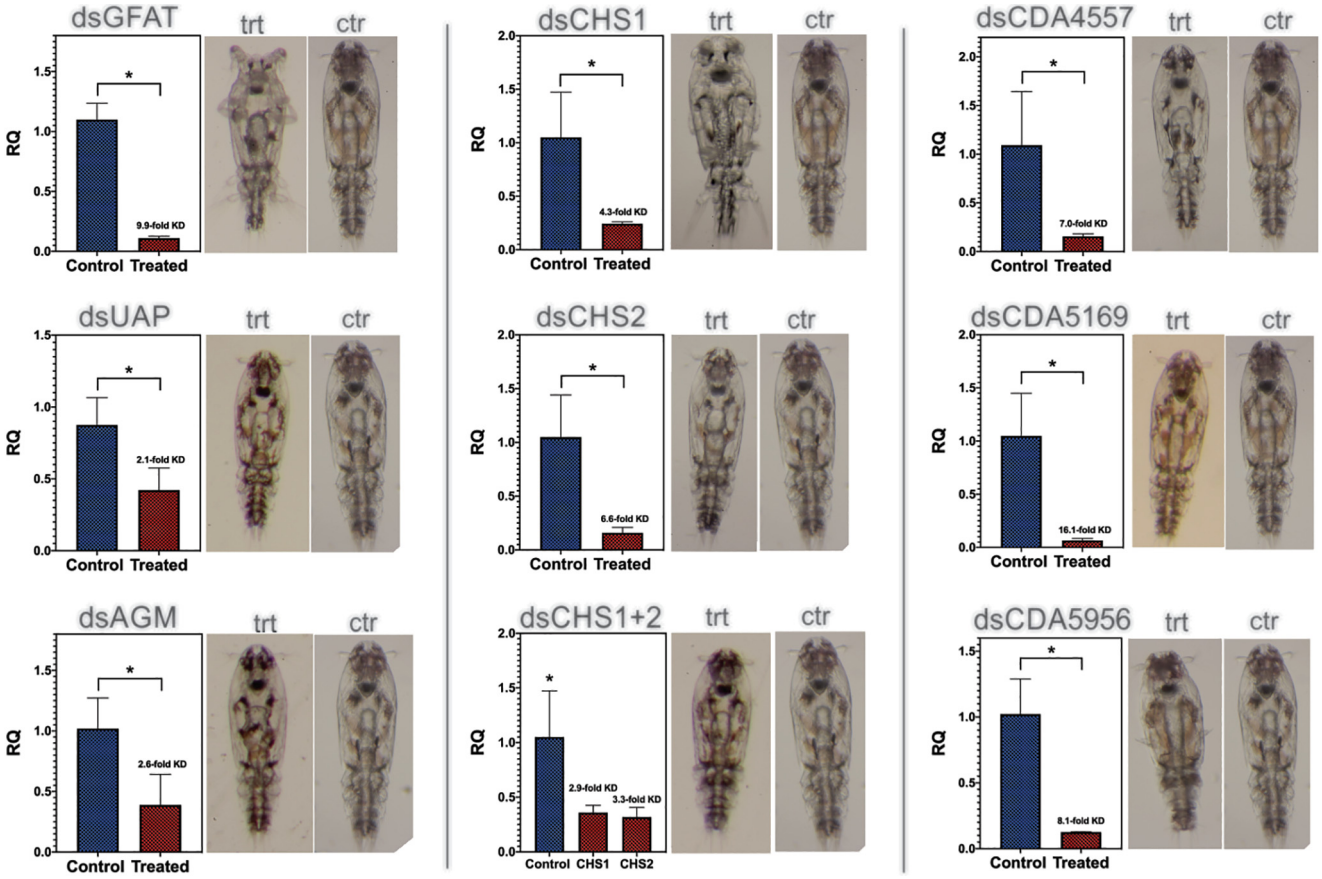

Fig. 1. Knockdown of *Lepeophtheirus salmonis* chitin synthesis pathway enzymes showing quantitative PCR verification of gene expression together with a representative image of the associated phenotype compared with that of the double-stranded cod trypsin (dsCPY) controls for reference. An asterisk (*) indicates a significant difference in expression between control (ctr) and treated (trt) *L. salmonis* normalised relative quantities.

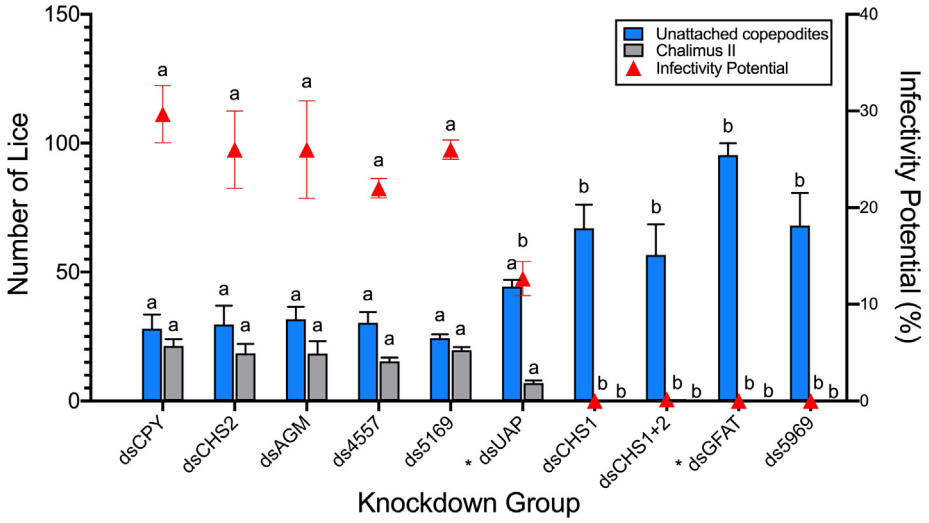

Fig. 2. Infectivity potential of double stranded RNA-treated *Lepeophtheirus salmonis*. The left *Y*-axis represents the number of lice collected from the effluent water during a 2 h period after infection challenge (blue bars), or chalimus II counted per fish at 13 or 21 days p.i. (Experiment 1 or Experiment 2, respectively; grey bars), while the right *Y*-axis represents the infectivity potential (N_{inf}) as described in section 3. Knockdown groups from Experiment 1 are indicated by an asterisk (*). Replicated results from double stranded control, Chitin synthase 1, Chitin synthase 2, and Chitin synthase 1 + 2 treatments are shown from Experiment 2 as there was no significant difference between these data from Experiment 1 and Experiment 2 (data not shown). One-way ANOVA with a post-hoc Tukey's honest significant difference test was completed to determine differences between treatments. Significant differences within groups over treatments are denoted by lowercase letters ($P < 0.05$).

using phylogenetic reconstruction, *LsCDA4557* has been identified as *LsCDA2* due to significant clustering with other CDA2s and the presence of all three domains required for CDA group I classification. they *LsCDA5169* and *LsCDA5956* are missing the 5′ CBD present for the CDA groups to which clustered, which is likely to be the result of incomplete sequences. Based on current phylogenetic

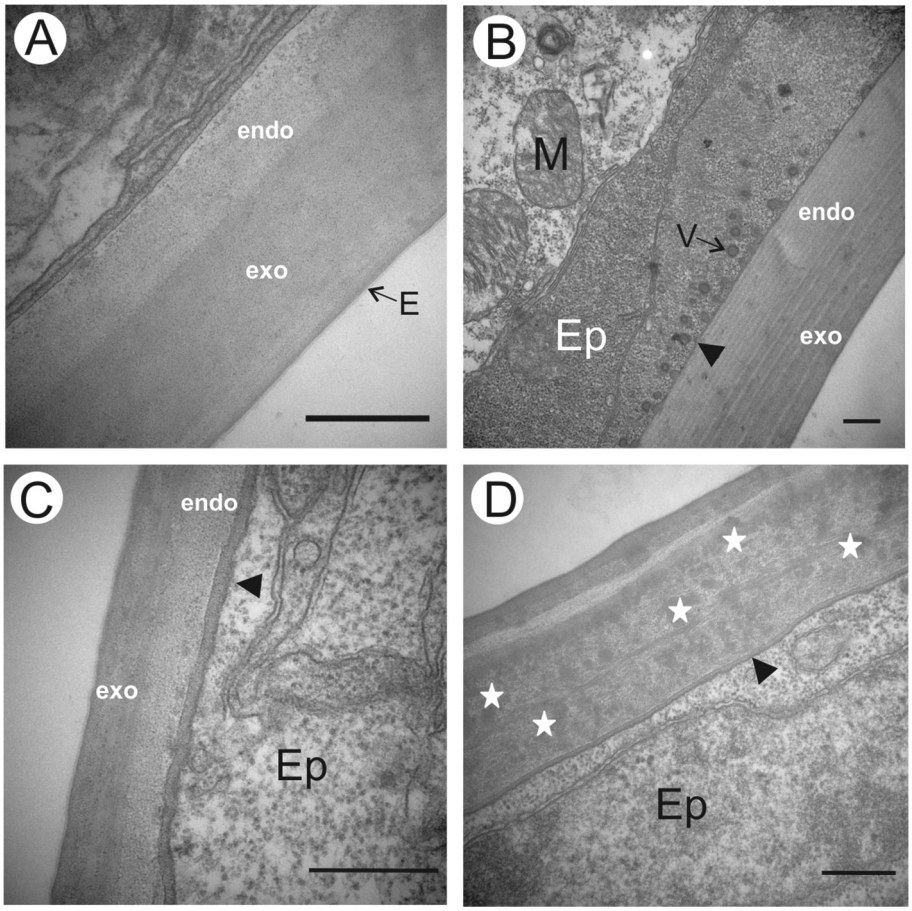

Fig. 3. Electron microscopy of *Lepeophtheirus salmonis* copepodites. (A) double-stranded cod trypsin (dsCPY)-treated lice at 60,000× magnification. (B) ds*UDP-N-acetylglucosamine pyrophosphorylase* (dsUAP)-treated lice at 10,000× magnification. (C) ds*Chitin synthase 1* (dsCHS1)-treated lice at 10,000× magnification. (D) ds*Glutamine: fructose-6-phosphate aminotransferase* (dsGFAT)-treated lice at 40,000× magnification. Scale bar represents 500 nm. E, new epicuticle; endo, endocuticle; exo, exocuticle; V, vesicles; M, mitochondrion; Ep, epithelium; electron-dense band (apical membrane) separating cuticle and Ep (AM; black arrow heads), electron-dense foci (white stars).

reconstruction, LsCDA*5169* and *LsCDA5956* can be putatively assigned as *LsCDA2b* and *LsCDA5*, respectively.

3.5. Knockdown validation and exploratory RT-qPCR

To confirm success of the RNAi treatment, pools (n = 2–8) of treated larvae (n = 20–100 larvae per pool) from the seven different treatments were assessed for transcript abundance. In addition to validating knockdown of target genes (*chitin synthase 1 (LsCHS1), chitin synthase 2 (LsCHS2), UDP acetylhexosamine pyrophosphorylase (LsUAP1), phosphoacetylglucosamine mutase (LsAGM), glutamine fructose-6-phosphate aminotransferase (LsGFAT1),* and *chitin deacetylases (LsCDA*), we assessed the transcript abundance of three genes in the putative chitin synthesis pathway: *chitinase 1 (LsCHI1*), *glucose-6-phosphate isomerase* (*LsGPI*), and *glucosamine-6-phosphate-N-acetyltransferase* (*LsGNA*).

Successful knockdown was inferred if there was a significant downregulation in expression of the target gene in the treatment group compared with the dsCPY185 control. We detected successful knockdown in all treatments (Fig. 1). However, as expected, there were varying degrees of knockdown, with some targets only achieving 2.1-fold reduction compared with controls, while others achieved 16.1-fold reduction.

By quantifying expression of all targets in each treatment group, we observed several apparent compensatory mechanisms (Fig. 6). For example, there was significant upregulation of *LsCHS1* in the dsUAP-treated group (P < 0.0001; Figs. 6, 7A), while the opposite was true in the dsCHS1-treated group with *LsUAP1* significantly upregulated (P < 0.0001; Figs. 6A, 7B). Knockdown of *LsUAP1* had a negative effect on infectivity potential (Fig. 2), but this phenotype was not as drastic as was observed in the *LsCHS1* knockdown group. The dsUAP treatment only resulted in a 2.1-fold reduction in expression compared with controls (Fig. 1), therefore in addition to significant upregulation of *LsCHS1,* it is possible that residual protein was sufficient, resulting in a normal phenotype.

Expression of *LsCHI1* was perturbed by knockdown of *LsCHS1+2* or *LsCHS2*, with significant reductions in expression after dsCHS1+2 and dsCHS2 treatment (P < 0.001 and P < 0.0001, respectively; Figs. 6, 7). Correlational analysis revealed an inverse relationship in expression of *LsCHI1* with that of *LsGFAT1, LsCHS1*, and all three *LsCDAs* (Fig. 6C).

Knockdown of *LsCDAs* also resulted in perturbation of expression of enzymes in the *L. salmonis* CSP (Figs. 6, 7). Of the three CDAs targeted in this study, *L. salmonis* appeared to be most sensitive to knockdown of *LsCDA5956,* resulting in severe phenotypic malformations and abrogation of infectivity (Fig. 2). Additionally, *LsGFAT1* and *LsCHS2* expression were significantly reduced in dsCDA5956-treated larvae. Furthermore, expression of *LsCHS1, LsGFAT1* and *LsCHI1* were negatively correlated with *LsCDA5956* (P < 0.00001; Fig. 7).

Neither the expression of *LsGNA* or *LsGPI* was significantly perturbed by any treatment, however, there were significant negative correlations in expression between *LsGNA* and *LsGFAT1*, *LsCHS1*, and *LsCDA5956* (P < 0.0001; Fig. 6).

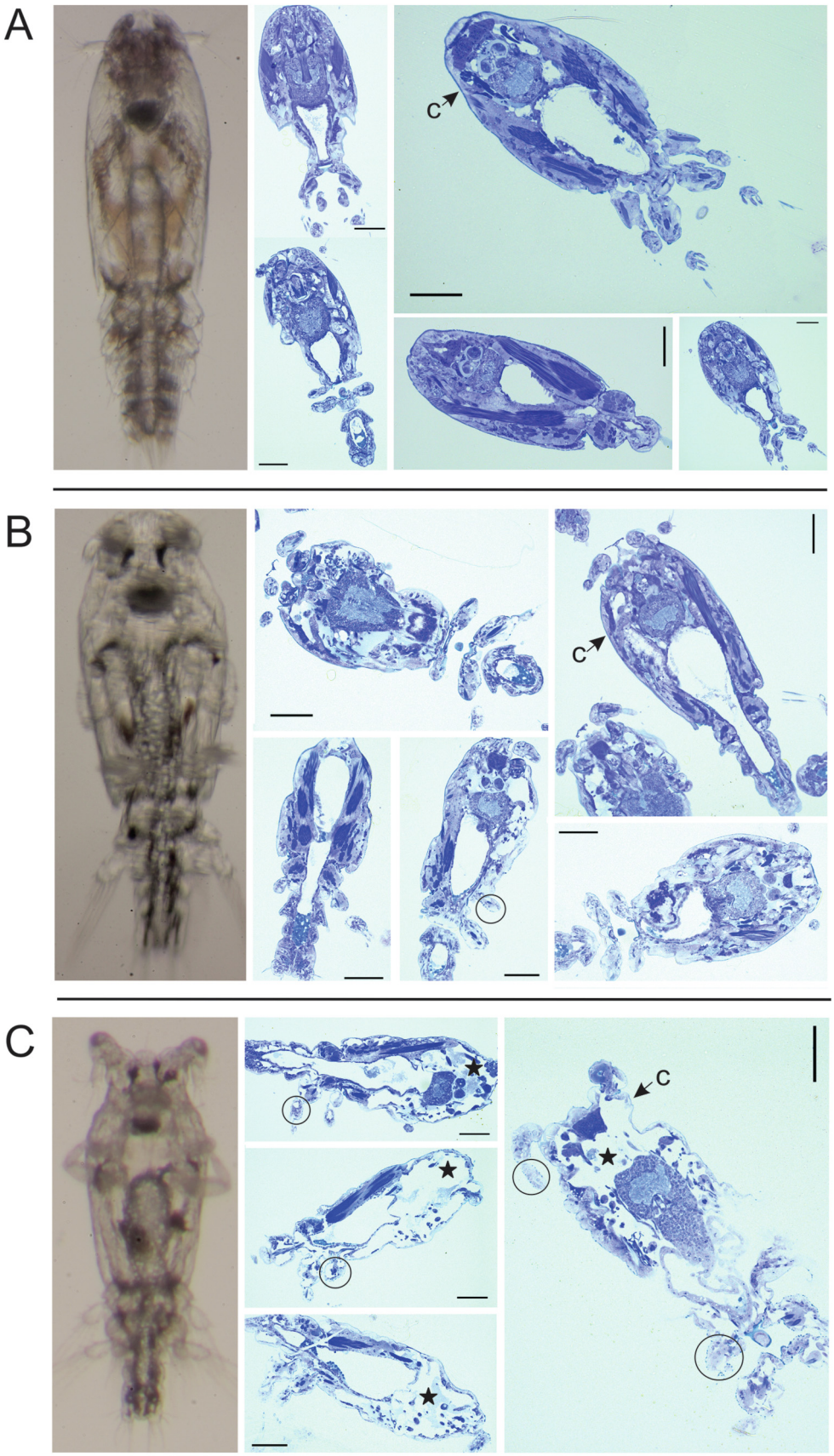

Fig. 4. Toluidine blue-stained sections of *Lepeophtheirus salmonis* copepodites viewed at 200× magnification. (A) double-stranded cod trypsin (dsCPY)-treated lice. (b) ds*Chitin synthase 1* (dsCHS1)-treated lice. (c) ds*Glutamine: fructose-6-phosphate aminotransferase* (dsGFAT)-treated lice. Scale bar represents 100 mm. c, cuticle; pockets of empty space within the exoskeleton are denoted by a star. Light-blue staining foci in appendages are circled.

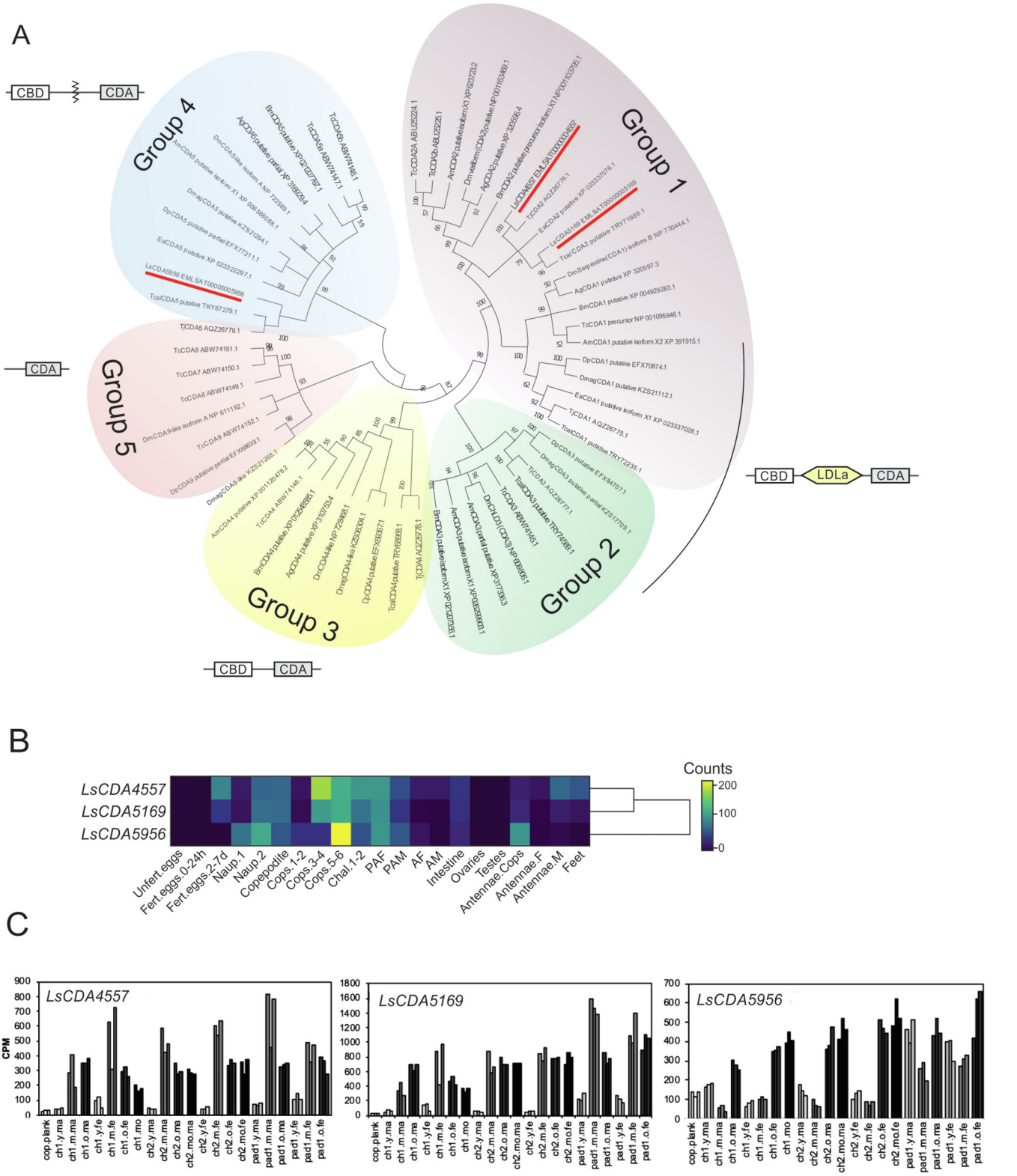

Fig. 5. Description of *Lepeophtheirus salmonis* CDAs. (A) Phylogenetic tree of putative Chitin Deacetylases (CDAs) from *L. salmonis*, *Drosophila melanogaster*, *Tribolium castaneum*, *Apis mellifera*, *Daphnia pulex*, *Daphnia magna*, *Tigriopus japonicus* and *Anopheles gambiae* constructed using MEGA X (v.10.1.7). A bootstrap analysis of 500 replicates was completed and values greater than 50% are displayed in the cladogram. *L. salmonis* CDAs are indicated in red. (B) Expression profiles of CDAs over developmental stages showing similar profiles between *LsCDA4557* and *LsCDA5169* expression, both clustering with Group 1 CDAs. Data obtained at licebase.org. Counts are in fragments per kilobase million (FKPM). (C) Expression profiles in counts per million (CPM) of *L. salmonis* CDAs showing the involvement of *LsCDA4557*, *LsCDA5169* and *LsCDA5956* during moulting over time.

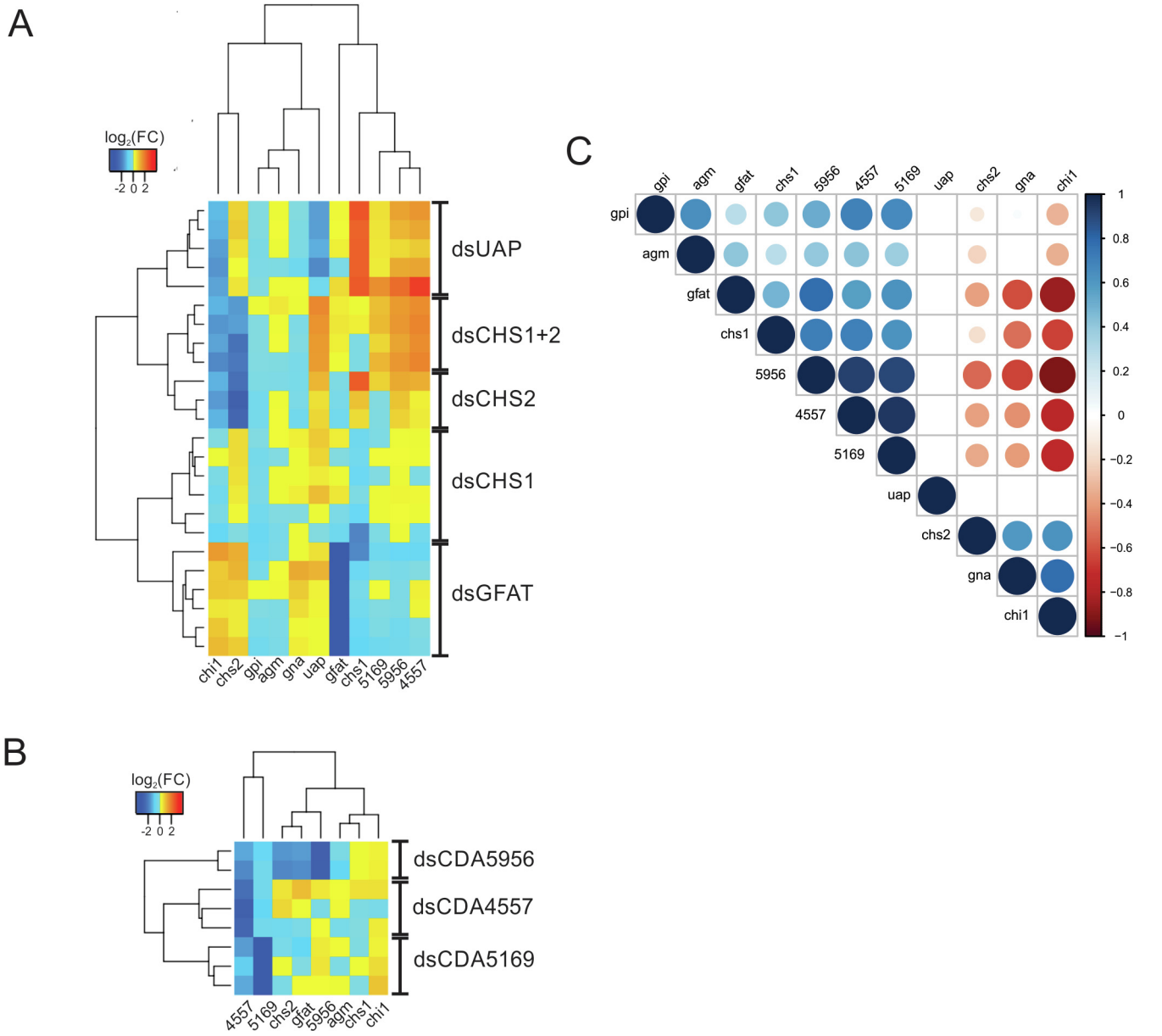

Fig. 6. Heatmap of $\log_2$-transformed expression for double stranded RNA treatments within the chitin synthesis pathway (A), or the chitin degradation pathway of *Lepeophtheirus salmonis* (B). Correlation matrix for all sample-gene combinations (C), showing Pearson's r correlation as positive (blue) or negative (red). Only significant correlations are shown ($P < 0.05$).

Transcripts within the *N*-glycosylation, GPI anchor biosynthesis and protein *O*-GlcNAcylation pathways were profiled to determine the potential impact of the dsRNA treatments on other essential molecular pathways. We observed significant differential expression in treated groups compared with dsCPY controls (Supplementary Fig. S1). For example, treatment with dsCHS1 resulted in significant upregulation of *LsOGT* ($P = 0.0002$), *LsPGAP1* ($P = 0.0004$), *LsPIGA* ($P = 0.0014$) and *LsPIGL* ($P = 0.004$), while *LsC1GALT1* was significantly downregulated ($P < 0.0001$). Treatment with dsCHS2 resulted in downregulation of *LsGANAB* ($P = 0.0008$), *LsMGAT2* ($P = 0.0031$), *LsC1GALT1* ($P = 0.0149$) and *LsPIGL* ($P < 0.0001$). The combination of dsCHS1 + 2 significantly upregulated *LsOGT* ($P = 0.0003$) and *LsPGAP1* ($P = 0.0177$), while *LsPIGL* ($P = 0.0188$) was downregulated. *LsC1GALT1* ($P < 0.0001$) and *LsOGT* ($P < 0.0001$) were upregulated while *LsPIGL* ($P < 0.0001$) was downregulated after dsGFAT treatment. Finally, treatment with dsUAP resulted in significant upregulation of *LsOGT* ($P < 0.0001$) and *LsPGAP1* ($P = 0.004$) while *LsPIGL* ($P < 0.0001$) was downregulated. *LsGCNT1*, *LsDPM1*, *Ls*ALG*13* and *LsGALNT* were not impacted by any of the dsRNA treatments.

4. Discussion

Similar to all other chitinous arthropods, salmon lice (*L. salmonis*) must periodically shed an exoskeleton in order to develop. This process is contingent upon a functional CSP, whereby old or new chitin molecules are incorporated into a new chitinous membrane. Despite the obvious importance of this pathway for physiology and fitness, very little is known about the molecular pathways involved in the CSP of *L. salmonis*.

Our observations suggest there are three points at which chitin synthesis in *L. salmonis* is sensitive to perturbations (Fig. 8). Firstly, *glutamine:fructose-6-phosphate aminotransferase* (*LsGFAT1*),

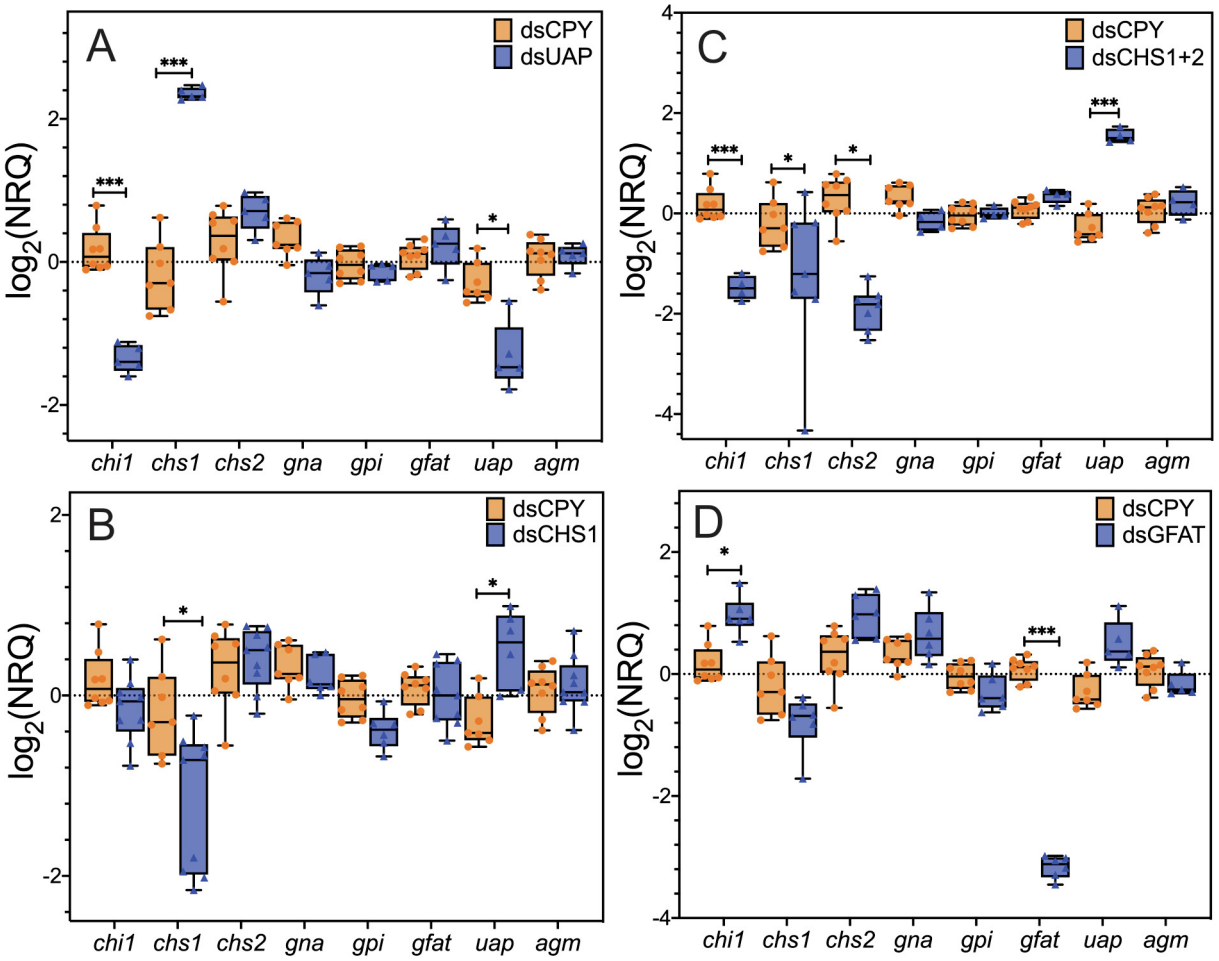

Fig. 7. Boxplots showing gene expression (log_2-transformed NRQs) of enzymes involved in the chitin synthesis pathway of *Lepeophtheirus salmonis* following double stranded RNA treatment of: (A) *LsUAP1*, (B) *LsCHS1*, (C) *LsCHS1+2* and (D) *LsGFAT*. Orange bars represent expression of the respective gene in the negative control (dsCPY), while the blue bars represent expression in the corresponding treatment group. One-way ANOVA with a post-hoc Tukey's honest significant difference test was used to detect significant differences in expression between the control and treatment groups (*$P < 0.01$, **$P < 0.001$, ***$P < 0.0001$).

whereby knockdown results in suppression of *LsCHS1* expression and upregulation of *LsCHI1* expression that is accompanied by severe phenotypic aberration, inability to swim and significantly reduced infectivity potential. Secondly, *chitin synthase 1* (*LsCHS1*), whereby gene expression knockdown results in upregulation of upstream *LsUAP1* and suppression of *LsCHI1* expression which impacts the normal physiology of swimming appendages and subsequent abrogation of infectivity. And lastly, a *chitin deacetylase* (*LsCDA5956; LsCDA5*), whereby gene expression knockdown has an inhibitory effect on both *LsGFAT1* expression and *LsCHS2* expression, as well as suppressing expression of another CDA (*LsCDA4557; LsCDA2*), and similarly disrupts normal physiology of the swimming appendages with a severe negative impact on proper swimming abilities compared with controls, and renders copepods unable to attach to the host. Although *UDP-N-acetylglucosamine pyrophosphorylase* knockdown did have a negative effect on infectivity, we are unable to draw conclusions about whether this point in the pathway is a sensitive one, due to the fact that knockdown was minimal (2.1-fold reduction) and the overall phenotype appeared consistent with the control, thus the role of *LsUAP1* as a critical point in the pathway requires further study.

Biosynthesis of chitin occurs either by degradation of cuticle-derived N-acetylglucosamine (GlcNAc) achieved by chitinases, by enzymatic synthesis of new chitin which is primarily regulated by glucosamine:fructose-6-phosphate aminotransferase (GFAT; Kato et al. (2002)), or through degradation by chitin deacetylases (Arakane et al., 2009). GFAT is a cytoplasmic enzyme and its activity has been detected in almost every organism and tissue investigated (Kato et al., 2006). In insects, control of GFAT expression is a key step in UDP-N-acetylglucosamine synthesis which is critical during moulting but is also important for synthesis of highly glycosylated proteins such as salivary gland glue proteins. High sequence homology of GFAT across phyla indicates conservation in function, which is exemplified by the sensitivity of GFAT expression to UDP-GlcNAc, the final product of the hexosamine pathway. This enzyme has recently been described in *L. salmonis* with high homology to other insects, including a GAT2 motif at the N-terminus (Harðardóttir et al., 2019b). We report a significant phenotypic aberration after knockdown of *LsGFAT1*, including a complete abrogation of infectivity potential. Interestingly, in dsGFAT-treated animals, there was a compensatory effect observed in the pathway with downregulation of the downstream enzyme *LsCHS1* and upregulation of the chitin degradative enzyme *LsCHI1*. Sensitivity of GFAT to feedback inhibition has been described (Kato et al., 2002). However, these efforts were not sufficient to rescue the pathway and resulting lice were severely compromised. Thus, this enzyme represents a critical point in regulation of chitin synthesis of *L. salmonis*, similar to reports in other arthropods (Huang et al., 2007). Interestingly, this latter study found GFAT knockdown severely inhibited blood feeding and egg production in the Ixodid

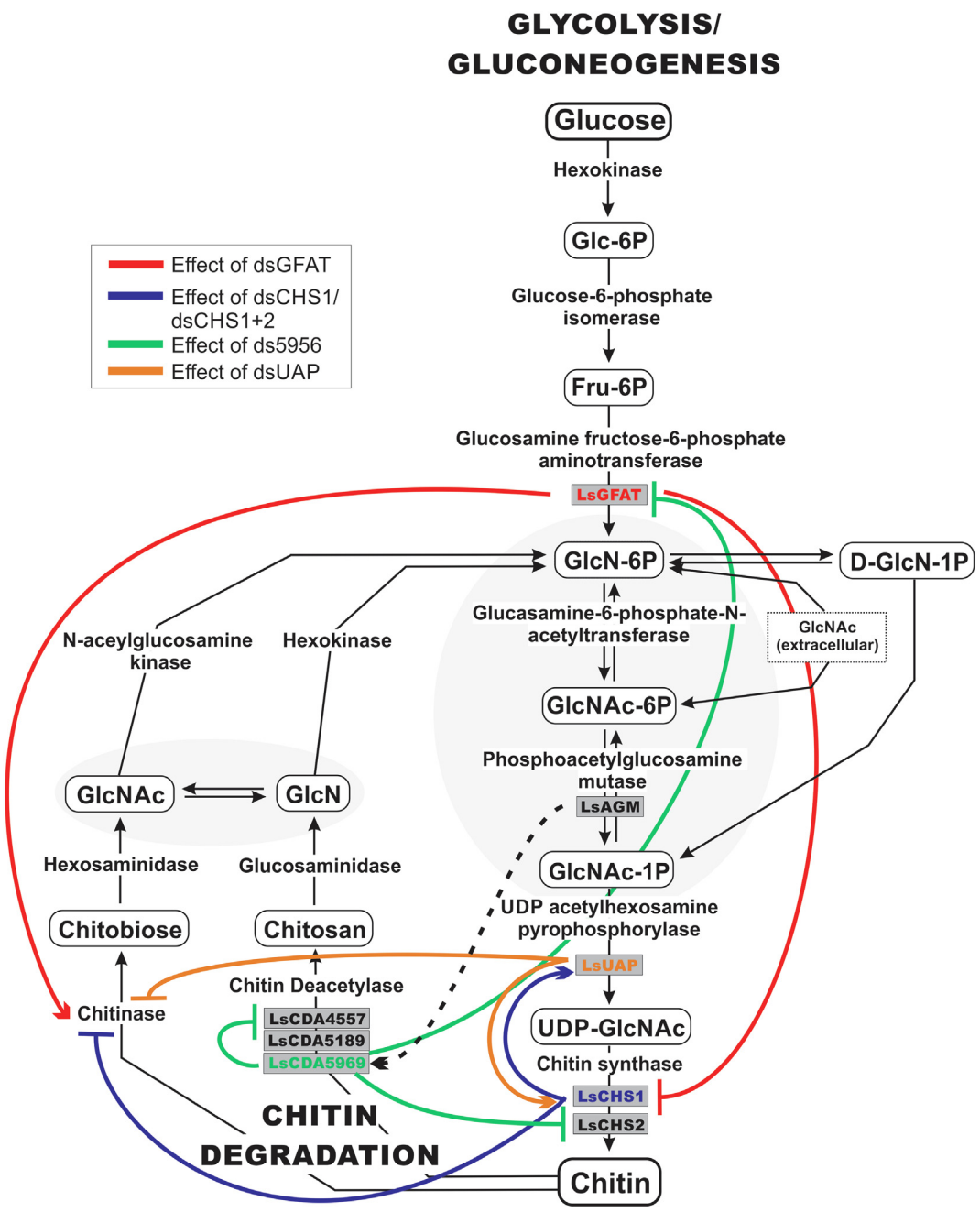

Fig. 8. Chitin synthesis pathway of *Lepeophtheirus salmonis* showing effects of double stranded RNA treatments on gene expression of other enzymes in the pathway. Only those treatments that resulted in phenotype aberrations following RNA interference (RNAi) are indicated. Points of the pathway that are within grey shaded areas are assumed to be less sensitive to perturbations as evidenced by a normal phenotype after RNAi. Adapted from Poley et al. (2018).

tick *Haemaphysalis longicornis*. These authors speculate that GFAT may also function to glycosylate salivary gland proteins involved in the host-parasite interaction (Huang et al., 2007). Unfortunately, the current study did not assess the effects of GFAT knockdown on adult *L. salmonis*; however, based on their similarities to ticks, it is certainly possible that *LsGFAT1* also functions during feeding. More experiments need to be conducted to confirm this hypothesis.

Similar to dsGFAT-treated animals, we observed extreme phenotypic malformations after treatment with dsCHS1. The majority of lice exhibited swollen cephalothorax and secondary antenna in addition to an inability to properly fold swimming legs under the posterior segment, representing a potential joint malformation as seen in knockdown studies involving *T. castaneum* (Arakane et al., 2004). Interestingly, dsCHS2 did not result in an aberrant phenotype and infectivity was similar to controls – only when dsCHS2 was co-administered with dsCHS1 was there an effect. Thus, similar to insects, *LsCHS2* does not appear to be required for successful moulting and cannot rescue the CSP in dsCHS1 individuals (Arakane et al., 2005). These results confirm earlier descriptions of the divergent functions and localization patterns of *LsCHS1* and *LsCHS2* (e.g., cuticle versus intestine, respectively (Harðardóttir et al., 2019b)). Moreover, there is evidence of stage-specific roles of different variants of CHS1 during moulting as shown for the red flour beetle *T. castaneum* (Arakane et al., 2005). Although we were unable to target different sequence variants of *LsCHS1* as they have not yet been identified, it is possible

that the dsCHS1 fragment targeted a variant that only effects a specific time during moult or developmental stage (i.e., copepodite versus pre-adult), or conversely, this treatment could have been targeting an exon common between different variants. Recently CHS1 has been proposed as the mode of action for BPUs in terrestrial arthropods, where researchers discovered a I1042M mutation in the *chitin synthase 1* gene of *Plutella xylostella* which confers resistance to BPUs. After utilising CRISPR-Cas9 to introduce this mutation into the orthologous *D. melanogaster* CHS1 (*kkv*) gene, the homozygous lines were found to have acquired BPU resistance (Douris et al., 2016). In contrast, there is no quantifiable impact of BPU exposure (lufenuron) on expression of CHS1 transcripts in either *L. salmonis* or *Caligus rogercresseyi* (an ectoparasitic copepod in the southern hemisphere) (Michaud, D., Poley, J., Koop, B., Mueller, A., Marin, S., Fast, M., 2018. Transcriptomic signatures of post-moult ageing and responses to lufenuron in copepodid sea lice (Caligus rogercresseyi), International Sea Lice Conference, 4–7 November, Peurto Varas, Chile; Poley et al., 2018). This may suggest: (i) BPUs operate at a posttranscriptional level, eliciting no relevant response on CHS transcripts; (ii) methods utilised (whole animal pooled extractions) might lack resolution to detect impacts at the transcriptional level; or (iii) BPUs might impact the copepod CSP differently compared with terrestrial arthropods. Thus, furthering our understanding of the copepod CSP will have profound impacts on the sustainability of the salmonid aquaculture industry as currently BPUs are the only chemical class to which resistance has not yet been reported in *L. salmonis* (Aaen et al., 2015), thus interactions involving the CSP will be crucial in screening for drug resistance and developing novel treatment strategies.

Interestingly, we observed a significant inverse relationship between expression of *LsCHS1* and *LsUAP1*. UDP acetylhexosamine pyrophosphorylase (UAP) is essential for production of UDP-GlcNAc, the building block of chitin, as well as for glycosylation of proteins, sphingolipids and secondary metabolites (Liu et al., 2013). We demonstrated successful but limited knockdown of *LsUAP1* which was accompanied by a significant induction of *LsCHS1* and downregulation of *LsCHI1*. However, these apparent compensatory mechanisms were not sufficient to prevent a reduction in infectivity in this group. Importantly, this decrease was only observed post-attachment as there was no difference in the number of dsUAP-treated lice flushed from the tanks during the infection challenge compared with controls. Only after attachment and/or moulting to chalimus was there a significant reduction in numbers.

A similar inverse relationship in expression was observed after dsCHS1 or dsCHS1+2 treatment, where there was upregulation of *LsUAP1*. In these two treatments, animals were severely compromised, with an inability to maintain buoyancy compared with controls, a lack of phototactic response and almost complete abrogation of infectivity. Interestingly, expression of the enzyme *LsCHI1* was downregulated in response to dsUAP and dsCHS1/dsCHS1+2, indicating that in these animals, there was an attempt to reduce degradation of chitin and maintain the current layer of cuticle. Furthermore, correlational analysis indicated an inverse regulation between *LsCHI1* and *LsGFAT1* or *LsCHS1*. This observation strengthens the proposed pathway, with *LsGFAT1* and *LsCHS1* as key enzymes in the synthesis pathway that are sensitive to perturbations in up- or downstream enzymes. For example, when *LsGFAT1* is reduced, our data suggests the pathway compensates and utilises a new substrate by increasing chitin degradation in order to maintain homeostasis in the pathway (Fig. 8). In a similar fashion, when *LsCHS1* is reduced, the system attempts to generate more substrate by upregulating *LsUAP1*, while suppressing expression of chitin degradation in order to maintain cuticular chitin. Interestingly, downregulation of *LsUAP1* did not inhibit CDA expression. This suggests that there are different utilisation pathways for chitobiose and chitosan, the degradative products of chitinase and CDAs, respectively.

CDAs have been categorised into five different groups based on conserved domains and general function. Group I (CDA1 and CDA2) and group II (CDA3) CDAs are identified by the presence of three conserved domains; a chitin-binding perithrophin-A domain (CBD), a low-density lipoprotein receptor class A domain (LDLa) and a CDA catalytic domain. Group III (CDA4) and Group IV (CDA5) CDAs lack the LDLa domain, with the latter group differing due to a large Ser/Thr/Pro/Gln-rich linker between these two domains. Lastly, Group V CDAs only contain a CDA domain and include CDA9s and *T. castaneum*-specific TcCDAs 6, 7 and 8 (Dixit et al., 2008; Muthukrishnan et al., 2012). The multiple variants of CDAs can be found throughout nearly all tissues of chitin-producing organisms and play an essential role in the reutilization of chitin (Zhao et al., 2010). In insects such as *D. melanogaster* and *T. castaneum*, CDAs play pivotal roles in development of the peritrophic membrane, femoral-tibial joint formation, tracheal tubes, elytrons and overall development (Arakane et al., 2005, 2009; Luschnig et al., 2006; Wang et al., 2006; Muthukrishnan et al., 2012). We did not observe a major impact on *L. salmonis* development, survival or infectivity after knockdown of putative *L. salmonis* CDA2s (*LsCDA4557* and *LsCDA5169*, 7- and 16.1-fold reduction, respectively). These results are in agreement with previous experiments assessing the impact of CDA2 knockdowns in *T. castaneum* which found there was no inhibition of moulting for any life stage when specifically suppressing expression of either *TcCDA2a* or *TcCDA2b*. However, ds*TcCDA2a* adults did suffer from impaired locomotion, evidenced by their inability to utilise the femoral-tibial joints, where they could not bend nor unbend the established leg position (Arakane et al., 2005). This phenotype is hypothesised to be the result of disruption in the ratio of chitin to chitosan in the joints produced by the hydrolyzation reaction of CDAs (Arakane et al., 2005; Dixit et al., 2008). Additionally, exon-specific ds*TcCDA2a/b* treated individuals had a reduction in egg-hatch rates but recovered from the parental RNAi effect 1–2 weeks later and larvae successfully moulted to the second instar. Based on phylogenetic reconstruction, *LsCDA4557* and *LsCDA5169* both belong to the CDA2 clade. Both CDAs clustered closely with other copepod putative CDA2s and together formed a sister group to insect CDA2s, which suggested these two putative CDA2s would behaviour similarly to *TcCDA2*s. Thus, we have demonstrated that putative *LsCDA2s* act similarly to CDA2s in insects such that moulting is not disrupted, however we were unable to confirm the presence of any aberrant phenotype in *L. salmonis*. *LsCDA4557* can confidently be annotated as an *LsCDA2* due to presence of all three domains typical to CDA2s; *LsCDA5169,* however, lacks a CBD domain. Therefore, it is probable the current sequence for *LsCDA5169* is missing an appreciable portion of the 5′ end. Further investigation into the sequence of *LsCDA5169* and number of variants of CDA2s present in *L. salmonis* is necessary to identify this group in its entirety.

CDA5s are the only other group to have two isoforms identified in arthropods (Arakane et al., 2005, 2009; Dixit et al., 2008; Muthukrishnan et al., 2012) and, similar to CDA2s, their diverse role is expected to be essential as their isoforms have been identified and are highly conserved with those identified in *T. castaneum*. CDA5s are primarily expressed in the cuticle throughout the body and at all life stages, with the exception of *TcCDA5b* whose transcripts were also detected in larval midguts (Arakane et al., 2009). However, expression knockdown of CDA5s does not result in any adverse consequences when investigated within *T. castaneum*. *LsCDA5956* has been putatively assigned as a group IV CDA5 based on our phylogenetic analysis, and interestingly produced a severe phenotype in *L. salmonis* which resembles that of the *TcCDA2a* isoform knockdown (Arakane et al., 2005), where

dsCDA5956-treated copepodites were unable to properly utilise their swimming appendages and the cephalothorax and secondary antennae were swollen. Exploratory qPCR revealed dsCDA5956-treated lice also had significantly reduced transcript levels of *LsCHS2* and, more importantly, *LsGFAT1*. Thus, it is probable that the negative phenotype was the result of reduced expression of both *LsCDA5956* and *LsGFAT1*.

Phylogenetic placement of *LsCDA5956* has proved difficult, similar to *LsCDA5169*. Only a CDA domain is present in this transcript and yet it clusters with other group IV CDAs. Furthermore, *LsCDA5956* appears to be a partial sequence and as such is significantly shorter than arthropod CDA5s (≥400 amino acids, (Dixit et al., 2008; Muthukrishnan et al., 2012)). Furthermore, other crustaceans including *D. magna, D. pulex* and *E. affinis* (Branchiopoda and Calanoida) did have both domains present, representing the conservation of both domains in Crustacea and Copepoda. Conversely, the complete coding region for *T. japonicus* CDA5 (KX427157.1) did not have a CBD present. Recent insights into the evolutionary history of Copepoda suggests Branchiopoda species are more closely related to Insecta than Copepoda, while within Copepoda, Siphonostomatoida (*L. salmonis*) and Harpacticoida (*T. japonicus* and *T. californicus*) are more closely related to each other than Calanoida (Eyun, 2017). Thus, as CDA information is currently limited for copepods, it is difficult to surmise whether certain linages have lost their chitin-binding perithrophin-A domain, or whether it is the result of incomplete sequence annotation. Based on the data currently available, *LsCDA5956* should be annotated as a putative *LsCDA5* and expression knockdown has demonstrated the potential for CDA5 to have an essential role in successful development and infectivity within a copepod species.

We observed a negative correlation in expression of *LsCHI1* to all three CDAs, providing additional support to our suggestion that there are different utilisation pathways for chitobiose and chitosan. We hypothesise this is primarily driven through a balance between the ratio of chitin to chitobiose and/or chitosan within a given tissue as downstream substrates of chitobiose and chitosan (GlcN and GlcNAc, respectively) are acetylated and/or deacetylated (EC 3.5.1.33/EC 2.3.13) into one another (Fig. 8; Dixit et al. (2008)). Thus, phenotypes associated solely with either chitinases or CDAs would be expected to be a direct result of the chitobiose/chitosan to chitin ratio. However, further work is required to elucidate this relationship.

Quantification of gene expression from transcripts within the *N*-glycosylation, GPI anchor biosynthesis and protein *O*-GlcNAcylation pathways were analysed to determine the impact dsRNA treatments may have had on other essential molecular pathways or whether chitin synthesis was prioritised. Overall the transcripts which appeared generally sensitive to perturbations of the CSP were *O-GlcNAc Transferase* which catalyses the addition of a *N*-acetylglucosamine through an *O*-glycosidic linkage, *glycoprotein-N-acetylgalactosamine 3-beta-galactosyltransferase* which generates a common precursor for many extended mucin-type *O*-glycan structures (Zeidan and Hart, 2010), and *phosphatidylinositol glycan anchor biosynthesis class L isoform C,* which catalyses the second step of GPI biosynthesis (Kinoshita and Norimitsu, 2000). Thus, RNAi of various transcripts along the CSP of *L. salmonis* appears to also impact alternate pathways associated with common substrates. Importantly, knockdown of *LsCHS1* appeared to have a pathway-specific effect on GPI biosynthesis. As UDP-GlcNAc is a common substrate for both chitin and GPI synthesis (Kinoshita and Norimitsu, 2000), reducing *LsCHS1* would likely make this substrate more available by decreasing synthesis of chitin and/or by increasing production via compensatory upregulation of *LsUAP1* (Fig. 8). Upregulation of GPI-GlcNAc transferases (*LsPIGL* and *LsPIGA*) in the pathway certainly suggests GPI biosynthesis activation; however, the contribution of this pathway as a compensatory mechanism to the CSP pathway will need to be further investigated to better understand any associations with the CSP. Interestingly, the GPI biosynthesis pathway is a therapeutic target against medically important parasites including *Trypanosoma brucei* (Ferguson et al., 1999).

In conclusion this is, to our knowledge, the first functional description of CDAs and identification of critical enzymes (*LsGFAT1*, *LsCHS1*, *LsCDA5956*) within the CSP of copepods. *LsCDA4557* and *LsCDA5169* are both putative CDA2s and did not result in any adverse phenotypes despite significant expression reduction. Knockdown of *LsCDA5956*, a putative CDA5, resulted in compromised swimming appendages which appeared to remain locked in an established position, swollen cephalothorax and secondary antenna, and complete elimination of infectivity potential. Furthermore, knockdown of *LsGFAT1* and *LsCHS1* resulted in similar abnormal phenotypes lacking successful development and infectivity, while *LsUAP1* knockdown had only a minor effect on infectivity. The complexity and potential for compensatory mechanisms within the chitin synthesis pathway cannot be overemphasised. Elucidation of the chitin synthesis and degradation pathway of *L. salmonis* will be essential for the sustainability of the salmonid aquaculture industry, as currently the only chemotherapeutics with no described resistance in lice are BPUs. Furthermore, identification of the difference in the mode of action of BPUs between Insecta and Copepoda (e.g., as *LsCHS1* and *CrCHS1* are not differentially expressed in response to BPUs) will be crucial for resistance screening and management strategies, and a clear understanding of the CSP in copepods will generate multiple targets for novel therapeutic discoveries.

Acknowledgements

This research was funded by Elanco Animal Health Canada, a Collaborative research and development grant through the Natural Sciences and Engineering Research Council (NSERC, Canada) (499789-2016), and by the Research Council of Norway, SFI-Sea Lice Research Centre (SLRC), grant number 203516/O30. We would like to thank Per Gunnar Espedal at the SLRC in Bergen for excellent help in the salmon louse facility. LMB and OOI were funded by the Canada Excellence Research Chairs (CERC, Canada), and LMB and DM by the Research Council of Norway and Norwegian Agency for International Cooperation and Quality Enhancement in Higher Education, grant number 249816 for travel to Norway to perform experiments at the SLRC.

Appendix A. Supplementary data

Supplementary data to this article can be found online at https://doi.org/10.1016/j.ijpara.2020.06.007.

References

Aaen, S.M., Helgesen, K.O., Bakke, M.J., Kaur, K., Horsberg, T.E., 2015. Drug resistance in sea lice: a threat to salmonid aquaculture. Trends Parasitol. 31, 72–81. https://doi.org/10.1016/j.pt.2014.12.006.

Arakane, Y., Baguinon, M.C., Jasrapuria, S., Chaudhari, S., Doyungan, A., Kramer, K.J., Muthukrishnan, S., Beeman, R.W., 2011. Both UDP N-acetylglucosamine pyrophosphorylases of *Tribolium castaneum* are critical for molting, survival and fecundity. Insect Biochem. Mol. Biol. 41, 42–50. https://doi.org/10.1016/j.ibmb.2010.09.011.

Arakane, Y., Dixit, R., Begum, K., Park, Y., Specht, C.A., Merzendorfer, H., Kramer, K.J., Muthukrishnan, S., Beeman, R.W., 2009. Analysis of functions of the chitin deacetylase gene family in *Tribolium castaneum*. Insect Biochem. Mol. Biol. 39, 355–365. https://doi.org/10.1016/j.ibmb.2009.02.002.

Arakane, Y., Hogenkamp, D.G., Zhu, Y.C., Kramer, K.J., Specht, C.A., Beeman, R.W., Kanost, M.R., Muthukrishnan, S., 2004. Characterization of two chitin synthase genes of the red flour beetle, *Tribolium castaneum*, and alternate exon usage in one of the genes during development. Insect Biochem. Mol. Biol. 34, 291–304. https://doi.org/10.1016/j.ibmb.2003.11.004.

Arakane, Y., Muthukrishnan, S., Kramer, K.J., Specht, C.A., Tomoyasu, Y., Lorenzen, M. D., Kanost, M., Beeman, R.W., 2005. The *Tribolium* chitin synthase genes TcCHS1 and TcCHS2 are specialized for synthesis of epidermal cuticle and midgut peritrophic matrix. Insect Mol. Biol. 14, 453–463. https://doi.org/10.1111/j.1365-2583.2005.00576.x.

Boxaspen, K., 2006. A review of the biology and genetics of sea lice. ICES J. Mar. Sci. 63, 1304–1316. https://doi.org/10.1016/j.icesjms.2006.04.017.

Bron, J.E., Shinn, A.P., Sommerville, C., 2000a. Ultrastructure of the cuticle of the chalimus larva of the salmon louse *Lepeophtheirus salmonis* (Krøyer, 1837) (Copepoda: Caligidae). Contrib. Zool. 69, 39–49. https://doi.org/10.1163/18759866-0690102004.

Bron, J.E., Shinn, A.P., Sommerville, C., 2000b. Moulting in the chalimus larva of the salmon louse *Lepeophtheirus salmonis* (Copepoda, Caligidae). Contrib. Zool. 69, 31–38. https://doi.org/10.1163/18759866-0690102003.

Brooker, A.J., Skern-Mauritzen, R., Bron, J.E., 2018. Production, mortality, and infectivity of planktonic larval sea lice, *Lepeophtheirus salmonis* (Kroyer, 1837): current knowledge and implications for epidemiological modelling. ICES J. Mar. Sci. 75, 1214–1234. https://doi.org/10.1093/icesjms/fsy015.

Carmichael, S.N., Bron, J.E., Taggart, J.B., Ireland, J.H., Bekaert, M., Burgess, S.T., Skuce, P.J., Nisbet, A.J., Gharbi, K., Sturm, A., 2013. Salmon lice (*Lepeophtheirus salmonis*) showing varying emamectin benzoate susceptibilities differ in neuronal acetylcholine receptor and GABA-gated chloride channel mRNA expression. BMC Genomics 14, 408. https://doi.org/10.1186/1471-2164-14-408.

Cohen, E., 2010. Chapter 2: chitin biochemistry: synthesis, hydrolysis and inhibition. In: Casas, J., Simpson, S.J. (Eds.), Advances in Insect Physiology: Insect Integument and Colour. Academic Press, London, Amsterdam, Oxford, Burlington, San Diego, pp. 5–74. https://doi.org/10.1016/S0065-2806(10)38005-2.

Dixit, R., Arakane, Y., Specht, C.A., Richard, C., Kramer, K.J., Beeman, R.W., Muthukrishnan, S., 2008. Domain organization and phylogenetic analysis of proteins from the chitin deacetylase gene family of *Tribolium castaneum* and three other species of insects. Insect Biochem. Mol. Biol. 38, 440–451. https://doi.org/10.1016/j.ibmb.2007.12.002.

Doucet, D., Retnakaran, A., 2012. Chapter 6: insect chitin. metabolism, genomics and pest management. In: Dhadialla, T.S. (Ed.), Advances in Insect Physiology. Academic Press, Oxford, London, Amsterdam, Waltham and San Diego, pp. 437–551. https://doi.org/10.1016/B978-0-12-391500-9.00006-1.

Douris, V., Steinbach, D., Panteleri, R., Livadaras, I., Pickett, J.A., Van Leeuwen, T., Nauen, R., Vontas, J., 2016. Resistance mutation conserved between insects and mites unravels the benzoylurea insecticide mode of action on chitin biosynthesis. Proc. Natl. Acad. Sci. 113, 14692–14697. https://doi.org/10.1073/pnas.1618258113.

Eichner, C., Dalvin, S., Skern-Mauritzen, R., Malde, K., Kongshaug, H., Nilsen, F., 2015a. Characterization of a novel RXR receptor in the salmon louse (*Lepeophtheirus salmonis*, Copepoda) regulating growth and female reproduction. BMC Genomics 16, 1–23. https://doi.org/10.1186/s12864-015-1277-y.

Eichner, C., Harasimczuk, E., Nilsen, F., Grotmol, S., Dalvin, S., 2015b. Molecular characterisation and functional analysis of LsChi2, a chitinase found in the salmon louse (*Lepeophtheirus salmonis salmonis*, Kroyer 1838). Exp. Parasitol. 151–152, 39–48. https://doi.org/10.1016/j.exppara.2015.01.011.

Eichner, C., Nilsen, F., Grotmol, S., Dalvin, S., 2014. A method for stable gene knockdown by RNA interference in larvae of the salmon louse (*Lepeophtheirus salmonis*). Exp. Parasitol. 140, 44–51. https://doi.org/10.1016/j.exppara.2014.03.014.

Eyun, S.I., 2017. Phylogenomic analysis of Copepoda (Arthropoda, Crustacea) reveals unexpected similarities with earlier proposed morphological phylogenies. BMC Evol. Biol. 17, 1–12. https://doi.org/10.1186/s12862-017-0883-5.

Felsentein, J., 1985. Confidence limits on phylogenies: an approach using the bootstrap. Evolution (N.Y) 39, 783–791.

Ferguson, M.A.J., Brimacombe, J.S., Brown, J.R., Crossman, A., Dix, A., Field, R.A., Güther, M.L.S., Milne, K.G., Sharma, D.K., Smith, T.K., 1999. The GPI biosynthetic pathway as a therapeutic target for African sleeping sickness. Biochim. Biophys. Acta - Mol. Basis Dis. 1455, 327–340. https://doi.org/10.1016/S0925-4439(99)00058-7.

Hamre, L.A., Eichner, C., Caipang, C.M.A., Dalvin, S.T., Bron, J.E., Nilsen, F., Boxshall, G., Skern-Mauritzen, R., 2013. The salmon louse *Lepeophtheirus salmonis* (Copepoda: Caligidae) life cycle has only two chalimus stages. PLoS One 8, 1–9. https://doi.org/10.1371/journal.pone.0073539.

Hamre, L.A., Glover, K.A., Nilsen, F., 2009. Establishment and characterisation of salmon louse (*Lepeophtheirus salmonis* (Kroyer 1837)) laboratory strains. Parasitol. Int. 58, 451–460. https://doi.org/10.1016/j.parint.2009.08.009.

Hamre, L.A., Nilsen, F., 2011. Individual fish tank arrays in studies of *Lepeophtheirus salmonis* and lice loss variability. Dis. Aquat. Organ. 97, 47–56.

Harðardóttir, H.M., Male, R., Nilsen, F., Dalvin, S., 2019a. Effects of chitin synthesis inhibitor treatment on *Lepeophtheirus salmonis* (Copepoda, Caligidae) larvae. PLoS One 14, 1–16. https://doi.org/10.1371/journal.pone.0222520.

Harðardóttir, H.M., Male, R., Nilsen, F., Eichner, C., Dondrup, M., Dalvin, S., 2019b. Chitin synthesis and degradation in *Lepeophtheirus salmonis*: molecular characterization and gene expression profile during synthesis of a new exoskeleton. Comp. Biochem. Physiol. -Part A Mol. Integr. Physiol. 227, 123–133. https://doi.org/10.1016/j.cbpa.2018.10.008.

Huang, X., Tsuji, N., Miyoshi, T., Motobu, M., Islam, M.K., Alim, M.A., Fujisaki, K., 2007. Characterization of glutamine: fructose-6-phosphate aminotransferase from the ixodid tick, *Haemaphysalis longicornis*, and its critical role in host blood feeding. Int. J. Parasitol. 37, 383–392. https://doi.org/10.1016/j.ijpara.2006.11.012.

Jones, D.T., Taylor, W.R., Thornton, J.M., 1992. The rapid generation of mutation data matrices from protein sequences. Comput. Appl. Biosci. 8, 275–282.

Kato, N., Dasgupta, R., Smartt, C.T., Christensen, B.M., 2002. Glucosamine:fructose-6-phosphate aminotransferase: gene characterization, chitin biosynthesis and peritrophic matrix formation in *Aedes aegypti*. Insect Mol. Biol. 11, 207–216. https://doi.org/10.1046/j.1365-2583.2002.00326.x.

Kato, N., Mueller, C.R., Fuchs, J.F., Wessely, V., Lan, Q., Christensen, B.M., 2006. Regulatory mechanisms of chitin biosynthesis and roles of chitin in peritrophic matrix formation in the midgut of adult *Aedes aegypti*. Insect Biochem. Mol. Biol. 36, 1–9. https://doi.org/10.1016/j.ibmb.2005.09.003.

Kinoshita, T., Norimitsu, I., 2000. Dissecting and manipulating the pathway for glycosylphosphatidylinositol anchor biosynthesis. Curr. Opin. Chem. Biol. 4, 632–638.

Kumar, S., Stecher, G., Li, M., Knyaz, C., Tamura, K., 2018. MEGA X: Molecular evolutionary genetics analysis across computing platforms. Mol. Biol. Evol. 35, 1547–1549. https://doi.org/10.1093/molbev/msy096.

Lee, J.B., Kim, H.S., Park, Y., 2017. Down-regulation of a chitin synthase a gene by RNA interference enhances pathogenicity of *Beauveria bassiana* ANU1 against *Spodoptera exigua* (HÜBNER). Arch. Insect Biochem. Physiol. 94, 1–11. https://doi.org/10.1002/arch.21371.

Liu, X., Cooper, A.M.W., Yu, Z., Silver, K., Zhang, J., Zhu, K.Y., 2019. Progress and prospects of arthropod chitin pathways and structures as targets for pest management. Pestic. Biochem. Physiol. 161, 33–46. https://doi.org/10.1016/j.pestbp.2019.08.002.

Liu, X., Li, F., Li, D., Ma, E., Zhang, W., Zhu, K.Y., Zhang, J., 2013. Molecular and functional analysis of UDP-N-acetylglucosamine pyrophosphorylases from the Migratory locust, *Locusta migratoria*. PLoS One 8. https://doi.org/10.1371/journal.pone.0071970.

Luschnig, S., Bätz, T., Armbruster, K., Krasnow, M.A., 2006. serpentine and vermiform encode matrix proteins with chitin binding and deacetylation domains that limit tracheal tube length in *Drosophila*. Curr. Biol. 16, 186–194. https://doi.org/10.1016/j.cub.2005.11.072.

Merzendorfer, H., 2013. Chitin synthesis inhibitors: old molecules and new developments. Insect Sci. 20, 121–138. https://doi.org/10.1111/j.1744-7917.2012.01535.x.

Merzendorfer, H., Zimoch, L., 2003. Chitin metabolism in insects: structure, function and regulation of chitin synthases and chitinases. J. Exp. Biol. 206, 4393–4412. https://doi.org/10.1242/jeb.00709.

Mio, T., Yamada-Okabe, T., Arisawa, M., Yamada-Okabe, H., 2000. Functional cloning and mutational analysis of the human cDNA for phosphoacetylglucosamine mutase: identification of the amino acid residues essential for the catalysis. Biochim. Biophys. Acta - Gene Struct. Expr. 1492, 369–376. https://doi.org/10.1016/S0167-4781(00)00120-2.

Muthukrishnan, S., Merzendorfer, H., Arakane, Y., Kramer, K.J., 2012. Chapter 7: Chitin metabolism in insects. In: Gilbert, L.I. (Ed.), Insect Molecular Biology and Biochemistry. Academic Press, London, Waltham and San Diago, pp. 193–235. https://doi.org/10.1016/B978-0-12-384747-8.10007-8.

Poley, J.D., Braden, L.M., Messmer, A.M., Igboeli, O.O., Whyte, S.K., Macdonald, A., Rodriguez, J., Gameiro, M., Rufener, L., Bouvier, J., Wadowska, D.W., Koop, B.F., Hosking, B.C., Fast, M.D., 2018. High level efficacy of lufenuron against sea lice (*Lepeophtheirus salmonis*) linked to rapid impact on moulting processes. Int. J. Parasitol. Drugs Drug Resist. 8, 174–188. https://doi.org/10.1016/j.ijpddr.2018.02.007.

Rozen, S., Skaletsky, H., 2000. Primer3 on the WWW for general users and for biologist programmers. Methods Mol. Biol. 132, 365–386.

Sandlund, L., Nilsen, F., Rune, M., Sussie, D., 2016. The ecdysone receptor (EcR) is a major regulator of tissue development and growth in the marine salmonid ectoparasite, *Lepeophtheirus salmonis* (Copepoda, Caligidae). Molecular & Biochemical Parasitology 208, 65–73. https://doi.org/10.1016/j.molbiopara.2016.06.007.

Urbina, M.A., Cumillaf, J.P., Paschke, K., Gebauer, P., 2019. Effects of pharmaceuticals used to treat salmon lice on non-target species: evidence from a systematic review. Sci. Total Environ. 649, 1124–1136. https://doi.org/10.1016/j.scitotenv.2018.08.334.

Wagner, G.N., Fast, M.D., Johnson, S.C., 2008. Physiology and immunology of *Lepeophtheirus salmonis* infections of salmonids. Trends Parasitol. 24, 176–183. https://doi.org/10.1016/j.pt.2007.12.010.

Wang, S., Jayaram, S.A., Hemphälä, J., Senti, K.A., Tsarouhas, V., Jin, H., Samakovlis, C., 2006. Septate-junction-dependent luminal deposition of chitin deacetylases restricts tube elongation in the *Drosophila* trachea. Curr. Biol. 16, 180–185. https://doi.org/10.1016/j.cub.2005.11.074.

Wootten, R., Smith, J., Needhama, E., 1982. Aspects of the biology of the parasitic copepods *Lepeophtheirus salmonis* and *Caligus elongatus* on farmed salmonids, and their treatment. Proc. R. Soc. Edinburgh. Sect. B. Biol. Sci. 81, 185–197. https://doi.org/10.1017/S0269727000003389.

Yang, W.J., Wu, Y.B., Chen, L., Xu, K.K., Xie, Y.F., Wang, J.J., 2015. Two chitin biosynthesis pathway genes in *Bactrocera dorsalis* (Diptera: Tephritidae): molecular characteristics, expression patterns, and roles in larval-pupal transition. J. Econ. Entomol. 108, 2433–2442. https://doi.org/10.1093/jee/tov186.

Zeidan, Q., Hart, G.W., 2010. The intersections between O-GlcNAcylation and phosphorylation: implications for multiple signaling pathways. J. Cell Sci. 123, 13–22. https://doi.org/10.1242/jcs.053678.

Zhao, X., Zhang, J., Zhu, K., 2019. Chito-protein matrices in arthropod exoskeletons and peritrophic matrices. In: Cohen, E., Merzendorfer, H. (Eds.), Extracellular Sugar-Based Biopolymers Matrices. Biologically-Inspired Systems, V12. Springer, Cambridge, pp. 3–56. https://doi.org/10.1007/978-3-030-12919-4_1.

Zhao, Y., Park, R.D., Muzzarelli, R.A.A., 2010. Chitin deacetylases: properties and applications. Mar. Drugs 8, 24–46. https://doi.org/10.3390/md8010024.